

## RESEARCH ARTICLE

# Novel exosome-targeted T-cell-based vaccine counteracts T-cell anergy and converts CTL exhaustion in chronic infection via CD40L signaling through the mTORC1 pathway

Rong Wang<sup>1,2</sup>, Aizhang Xu<sup>1</sup>, Xueying Zhang<sup>1,2</sup>, Jie Wu<sup>1</sup>, Andrew Freywald<sup>3</sup>, Jianqing Xu<sup>4</sup> and Jim Xiang<sup>1,2,5</sup>

CD8<sup>+</sup> cytotoxic T lymphocyte (CTL) exhaustion is a chief issue for ineffective virus elimination in chronic infectious diseases. We generated novel ovalbumin (OVA)-specific OVA-Exo and HIV-specific Gag-Exo vaccines inducing therapeutic immunity. To assess their therapeutic effect in chronic infection, we developed a new chronic infection model by i.v. infecting C57BL/6 mice with the OVA-expressing adenovirus AdVova. During chronic AdVova infection, mouse CTLs were found to express the inhibitory molecules programmed cell-death protein-1 (PD-1) and lymphocyte-activation gene-3 (LAG-3) and to be functionally exhausted, showing a significant deficiency in T-cell proliferation, IFN- $\gamma$  production and cytolytic effects. Naive CD8<sup>+</sup> T cells upregulated inhibitory PD-ligand 1 (PD-L1), B- and T-lymphocyte attenuator and T-cell anergy-associated molecules (Grail and Itch) while down-regulating the proliferative response upon stimulation in mice with chronic infection. Remarkably, the OVA-Exo vaccine counteracted T-cell anergy and converted CTL exhaustion. The latter was associated with (i) the upregulation of a marker for CTL functionality, diacetylated histone-H3 (diAcH3), (ii) a fourfold increase in CTLs, occurring independent of host DCs or CD4<sup>+</sup> T cells, and (iii) the restoration of CTL IFN- $\gamma$  production and cytotoxicity. *In vivo* OVA-Exo-stimulated CTLs upregulated the activities of the mTORC1 pathway-related molecules Akt, S6, eIF4E and T-bet, and treatment of the CTLs with an mTORC1 inhibitor, rapamycin, significantly reduced the OVA-Exo-induced increase in CTLs. Interestingly, OVA-Exo-mediated CD40L signaling played a critical role in the observed immunological effects. Importantly, the Gag-Exo vaccine induced Gag-specific therapeutic immunity in chronic infection. Therefore, this study should have a serious impact on the development of new therapeutic vaccines for human immunodeficiency virus (HIV-1) infection.

*Cellular & Molecular Immunology* (2017) 14, 529–545; doi:10.1038/cmi.2016.23; published online 6 June 2016

**Keywords:** anti-CD40 Ab; CD40L signaling; chronic infection; CTL exhaustion; HIV Gag; mTORC1 pathway; T-cell anergy; therapeutic T-cell vaccine

## INTRODUCTION

CD8<sup>+</sup> cytotoxic T lymphocytes (CTLs) are important effector T cells that are actively involved in the immune response against various viral infections. Following an acute viral infection, CTL immunity develops in three phases: expansion, contraction and memory.<sup>1</sup> In brief, the initial encounter with viral antigens (Ags) derived from an infectious agent triggers

the activation and proliferation of Ag-specific CTLs.<sup>2,3</sup> CTL responses often peak 7 days after an infection, followed by the contraction phase, when the majority (>90%) of effector CTLs (eCTLs) dies of activation-induced cell death.<sup>4,5</sup> The remaining 5–10% of the CTLs go on to seed the memory pool and become long-term memory CTLs (mCTLs).<sup>6</sup> These mCTLs are capable of responding robustly upon re-encounter with the

<sup>1</sup>Cancer Research Cluster, Saskatchewan Cancer Agency, Saskatoon, Saskatchewan, Canada S7N4H4; <sup>2</sup>School of Public Health, University of Saskatchewan, Saskatoon, Saskatchewan, Canada S7N 5E5; <sup>3</sup>Department of Pathology, College of Medicine, University of Saskatchewan, Saskatoon, Saskatchewan, Canada S7N 5E5; <sup>4</sup>Shanghai Public Health Clinical Center, Fudan University, Shanghai 201508, China and <sup>5</sup>Department of Oncology, College of Medicine, University of Saskatchewan, Saskatoon, Saskatchewan, Canada S7N 5E5

Correspondence: Dr J Xiang, Professor of Oncology, University of Saskatchewan, 4D30.1, Health Science Building, 107 Wiggins Road, Saskatoon, Saskatchewan, Canada S7N 5E5.

E-mail: jim.xiang@usask.ca

Received: 28 January 2016; Revised: 25 March 2016; Accepted: 25 March 2016

same viral Ags. In patients with chronic human immunodeficiency virus (HIV) infection, the immune system is often functionally deficient. For example, patients with progressive HIV infection often have CD4<sup>+</sup> T-cell deficiency and dysfunctional dendritic cells (DCs) due to the binding of the HIV Gp120 protein to CD4 on CD4<sup>+</sup>CCR5<sup>+</sup> T cells and the C-type lectin DC-SIGN on DCs, leading to CD4<sup>+</sup> T-cell death and the impairment of DCs by the viral cytopathic effect.<sup>7–10</sup> In addition, Ag-specific CD8<sup>+</sup> T cells that initially acquired effector function also gradually lose their functionality as chronic HIV infection progresses. This loss of function, known as ‘exhaustion,’ is hierarchical, with properties such as proliferative potential and IL-2 production affected early and IFN- $\gamma$  production reduced later in the course of infection.<sup>11,12</sup> T-cell exhaustion is probably one of the chief issues leading to ineffective virus control in HIV patients.

Previous therapeutic vaccines (using peptides, DNA or AdV vectors) requiring the engagement of the host DCs and CD4<sup>+</sup> T cells often failed to stimulate therapeutic immunity.<sup>13</sup> Distinct from these small biologic molecules, immune cell-based therapeutics have become a new third pillar of therapeutics. DCs are the most potent antigen-presenting cells (APCs). They have been used as vaccines to stimulate HIV-specific CTL responses in animal models<sup>14–16</sup> as well as in clinical trials on HIV patients.<sup>17–21</sup> In these trials, the safety profile has been excellent, with minor local side-effects observed. However, the immunotherapeutic efficacy of DC vaccines was found to be relatively poor in HIV patients with a deficiency in CD4<sup>+</sup> T-cell help. Nevertheless, some inhibitory effects on viral titers and disease progression have been found,<sup>19–21</sup> warranting a search for more potent cell-based HIV-specific therapeutic vaccines.

We previously developed a new ‘T-APC’ concept by demonstrating that CD4<sup>+</sup> helper T cells became ‘T-APCs’ capable of directly stimulating CD8<sup>+</sup> CTL responses after acquiring Ag-specific DC membrane molecules.<sup>22</sup> On the basis of this concept, we developed a novel ovalbumin (OVA)-specific, DC (DC<sub>OVA</sub>)-released, exosome (EXO)-targeted, T-cell-based (OVA-TEXO) vaccine expressing various cytokines such as IL-2, TNF- $\alpha$  and IFN- $\gamma$ <sup>23,24</sup> and demonstrated that non-specific T cells with uptake of Ag-specific, DC-released EXO via a CD54/LFA-1 interaction were able to directly stimulate Ag-specific CTL responses in the absence of CD4<sup>+</sup> T-cell help.<sup>23,24</sup> The OVA-TEXO vaccine acts more potently than the DC<sub>OVA</sub> approach by counteracting CD4<sup>+</sup>25<sup>+</sup>FoxP3<sup>+</sup> regulatory T (Treg) cell suppression.<sup>23,24</sup> To develop an HIV-specific T-cell-based vaccine, we constructed a recombinant HIV Gp120-expressing adenoviral vector (AdV<sub>Gp120</sub>) and generated a Gp120-specific Gp120-TEXO vaccine using AdV<sub>Gp120</sub>.<sup>25</sup> We found that the Gp120-TEXO vaccine stimulated Gp120-specific CTL responses, leading to therapeutic immunity.<sup>25,26</sup> Because HIV Gag is more suitable than Gp120 for vaccine-induced CTL immunity against HIV,<sup>27</sup> we developed an HIV Gag-specific, EXO-targeted, T-cell-based (Gag-TEXO) vaccine using AdV<sub>Gag</sub> and showed that the Gag-TEXO vaccine was capable of activating Gag-specific CTL

responses and immunity in transgenic HLA-A2 mice.<sup>28</sup> To enhance its immunogenicity, we generated a 4-1BBL-expressing Gag-TEXO vaccine and demonstrated that it elicited more efficient CTL responses and therapeutic immunity against Gag-expressing tumor challenges than our original Gag-TEXO vaccine.<sup>29</sup>

In this study, we initially infected C57BL/6 mice with the OVA-expressing adenovirus AdV<sub>Ova</sub> to establish a mouse AdV-induced chronic infection model. Two months after AdV infection, we assessed OVA-specific CTL responses by flow cytometry. We found that OVA-specific memory CTLs expressing CD40 along with the inhibitory programmed cell-death protein-1 (PD-1) and inhibitory lymphocyte-activation gene 3 (LAG-3) proteins and were functionally exhausted, which was indicative of an OVA-specific chronic infection in AdV<sub>Ova</sub>-infected mice. In addition, naive CD8<sup>+</sup> T cells expressed CD40, inhibitory programmed death-ligand 1 (PD-L1) and B- and T-lymphocyte attenuator (BTLA) molecules<sup>30</sup> and became anergic in mice with AdV<sub>Ova</sub>-induced chronic infection. To assess the immunogenicity of a 4-1BBL-expressing OVA-TEXO (termed OVA-TEXO) vaccine, C57BL/6 mice were infected with the  $\beta$ -galactosidase (Gal)-expressing adenovirus AdV<sub>Gal</sub>, which also creates a chronic infection model, showing rapid functional exhaustion and CTL deletion.<sup>31</sup> Some of these mice were immunized with the OVA-TEXO vaccine. Interestingly, our work revealed that OVA-TEXO vaccine stimulated potent CD8<sup>+</sup> T-cell responses in an AdV<sub>Gal</sub>-induced chronic infection model by counteracting naive CD8<sup>+</sup> T-cell anergy. To assess the potential conversion of CTL exhaustion by OVA-TEXO, AdV<sub>Ova</sub>-infected C57BL/6 mice were immunized with the OVA-TEXO vaccine. Our experiments showed that OVA-TEXO directly converted CTL exhaustion independent of the host CD4<sup>+</sup> T cells and DCs via the activation of the mTORC1 pathway. Consistent with this, treatment of CTLs with an mTORC1 inhibitor, rapamycin, significantly reduced the proliferation of functionally exhausted CTLs upon OVA-TEXO stimulation. Furthermore, our observations revealed that OVA-TEXO signaling through CD40L played a critical role in these immunological effects. To examine whether the Gag-TEXO vaccine is capable of effectively stimulating Gag-specific immune responses in chronic infection, we immunized AdV<sub>Ova</sub>-infected C57BL/6 mice with the HIV Gag-specific Gag-TEXO vaccine and determined that this vaccination induced therapeutic immunity against Gag-expressing tumors in chronic infection.

## MATERIALS AND METHODS

### Reagents, cell lines and animals

OVA was obtained from Sigma (St Louis, MO, USA). The OVA<sub>I</sub> (OVA<sub>257–264</sub>, SIINFEKL) peptide (H-2K<sup>b</sup>-restricted OVA antigen epitope) and Mut1 (FEQNTAQP) peptide (H-2K<sup>b</sup>-restricted tumor antigen epitope of an irrelevant 3LL lung carcinoma) were synthesized by Multiple Peptide Systems (San Diego, CA, USA). Biotin-labeled antibodies (Abs) specific for CD44 (IM7) and CD40 (3/23) and phycoerythrin (PE)-CD45RA (14.8) and PE/Cy5-anti-IFN- $\gamma$  (XMG1.2) Abs

were obtained from BD Biosciences (Mississauga, ON, Canada). Biotin-labeled Abs against CD62L (MEL-14), IL-7R (SB/199), lymphocyte-activation gene 3 (LAG-3) (C9B7W), diacetylated histone 3 (diAcH3) (Poly6019), and T-bet (Poly6235) and PE/Cy5-conjugated streptavidin were obtained from Biologend (San Diego, CA, USA). FITC- or PE/Cy5-CD8 (53-6.7) and biotin-labeled programmed cell-death protein 1 (PD-1) (J43), programmed death-ligand 1 (PD-L1) (1-111A), BTLA (8F4) and Ki67 (SolA15) Abs were obtained from eBioscience (San Diego, CA). Anti-phospho-Akt (pAkt) 1/2/3 (Ser 473), GRAIL (H-91) and ITCH (H-110) were obtained from Santa Cruz Biotechnology, Inc. (Dallas, TX, USA). Anti-phospho-eukaryotic translation initiation factor 4E (peIF4E) (Ser209), anti-phospho-S6 (pS6) ribosomal protein (Ser235/236) (D57.2.2E) and anti- $\beta$ -Actin (D6A8) polyclonal Abs were obtained from Cell Signaling Technology, Inc. (Danvers, MA, USA). PE-labeled H-2K<sup>b</sup>/OVA<sub>257-264</sub> tetramer (YTS 169.4) was obtained from Beckman Coulter (Miami, FL, USA). Fluorescein isothiocyanate (FITC)-labeled CD8 (53-6.7) was obtained from Caltag, Burlingame, CA, USA. FITC-conjugated AffiniPure goat anti-rabbit IgG (H+L) was obtained from Jackson ImmunoResearch Laboratories, Inc. (West Grove, PA, USA). Carboxyfluorescein succinimidyl ester (CFSE) was obtained from Molecular Probes (Eugene, OR, USA). The depleting anti-CD4 antibody was purified from the ascites of the hybridoma cell line GK1.5. Rat anti-mouse PD-L1 (10F.9G2) was obtained from BioXCell, Inc. (West Lebanon, NH, USA).<sup>32</sup> The recombinant adenoviral vectors AdVova, AdV<sub>Gal</sub>, AdV<sub>Gag</sub> and AdV<sub>41BBL</sub>, expressing OVA,  $\beta$ -galactosidase (Gal), HIV-1 Gag and 41BBL, respectively, were previously constructed in our laboratory.<sup>29,33</sup> Recombinant *Listeria monocytogenes* rLmOVA<sup>34</sup> expressing OVA was obtained from DMX Inc. (West Chester, PA, USA). The highly lung metastatic OVA-expressing BL6-10<sub>OVA</sub> and Gag-expressing BL6-10<sub>Gag</sub> tumor cell lines were generated in our lab.<sup>22,33</sup> Female wild-type (WT) C57BL/6 (B6), OVA-specific CD8<sup>+</sup> and CD4<sup>+</sup> T-cell receptor (TCR)-transgenic (Tg) OTI and OTII, transgenic diphtheria toxin receptor (DTR)-CD11c and various gene knockout (KO) mice were obtained from Jackson Laboratory (Bar Harbor, MA, USA). The animals were housed in the University of Saskatchewan Animal Facility (accreditation SCA-001). All experiments were performed according to protocols and guidelines approved by the Animal Research Ethics Board, University of Saskatchewan (Protocol# 20130020).

### Dendritic cell and exosome preparations

Bone marrow-derived DCs were obtained by culturing bone marrow cells from WT B6 mice in culture medium containing granulocyte monocyte colony-stimulating factor (GM-CSF) (20 ng/ml) and IL-4 (20 ng/ml) for 6 days as previously described.<sup>24</sup> The DCs were pulsed with OVA (0.5 mg/ml) overnight or infected with AdV<sub>Gag</sub> and termed DC<sub>OVA</sub> or DC<sub>Gag</sub> cells. DC<sub>OVA</sub> or DC<sub>Gag</sub>-released exosomes (EXO<sub>OVA</sub> or EXO<sub>Gag</sub>) were then purified from DC<sub>OVA</sub> or DC<sub>Gag</sub> culture supernatants by differential ultracentrifugation.<sup>24</sup>

### T-cell preparation

Naive or memory CD8<sup>+</sup> T cells were isolated from naive or AdV<sub>Gag</sub>- or AdVova-infected WT B6 and OVA-specific TCR transgenic OTI mouse spleens, enriched by passage through nylon wool columns (C&A Scientific, Manassas, VA, USA), and purified by negative selection using anti-mouse CD4 paramagnetic beads (DYNAL, Lake Success, NY, USA). To generate active CD8<sup>+</sup> T cells, the spleen cells from naive C57BL/6 mice were cultured in RPMI 1640 medium containing IL-2 (20 U/ml) and ConA (1  $\mu$ g/ml) for 3 days. CD8<sup>+</sup> T cells were then purified from ConA-activated T (ConA-T) cells using MACS anti-CD8 microbeads (Miltenyi Biotech, Auburn, CA, USA) to yield T-cell populations with > 98% purity.<sup>22</sup> ConA-T cells derived from IL-2, TNF- $\alpha$  and CD40L KO mice were termed (IL-2<sup>-/-</sup>), (TNF- $\alpha$ <sup>-/-</sup>) and (CD40L<sup>-/-</sup>) ConA-T cells, respectively.

### Preparation of OVA-Texo and Gag-Texo vaccines

OVA- and Gag-specific T-cell-based vaccines were generated by the incubation of CD8<sup>+</sup> ConA-T cells with EXO<sub>OVA</sub> and EXO<sub>Gag</sub> and subsequent transfection with AdV<sub>4-1BBL</sub>, as previously described.<sup>29</sup> The 41BBL-expressing, Gag-specific, T-cell-based vaccine is termed Gag-Texo, whereas the 41BBL-expressing, OVA-specific, T-cell-based vaccine is termed OVA-Texo. The 4-1BBL-expressing OVA-Texo cells derived from WT B6, (IL-2<sup>-/-</sup>), (TNF- $\alpha$ <sup>-/-</sup>) and (CD40L<sup>-/-</sup>) -ConA-T cells were termed OVA-Texo, and OVA-Texo (IL-2<sup>-/-</sup>), OVA-Texo(TNF- $\alpha$ <sup>-/-</sup>) and OVA-Texo(CD40L<sup>-/-</sup>) vaccines lacking IL-2, TNF- $\alpha$  and CD40L, respectively.

### Establishment of a chronic infection animal model

To establish an acute infection animal model, we infected B6 mice i.v. with rLmOVA (2000 c.f.u./mouse).<sup>34</sup> To establish a chronic infection animal model, we infected these B6 mice with AdVova (2  $\times$  10<sup>6</sup> p.f.u./mouse) or AdV<sub>Gal</sub> (1  $\times$  10<sup>8</sup> p.f.u./mouse), followed by a kinetic study of OVA-specific CD8<sup>+</sup> T-cell responses by flow cytometry. Mouse blood samples were collected at different time points post immunization and either double stained with FITC-anti-CD8 antibody (FITC-CD8) and PE-H-2K<sup>b</sup>/OVA<sub>257-264</sub> tetramer (PE-tetramer) or triple stained with FITC-CD8, PE-tetramer and PE-Cy5-antibodies for various immune molecules, and then the cells were analyzed by flow cytometry. For intracellular staining, the splenocyte samples were re-stimulated with 2  $\mu$ M OVAI peptide and subjected to intracellular staining (BD Biosciences) for IFN- $\gamma$ , as described previously.<sup>35</sup> To assess CTL recall responses, mouse splenic T-cell populations (containing mCTLs) from the chronically and acutely infected mice were adoptively transferred into WT B6 mice, and then the mice with similar amounts of adoptive mCTLs were i.v. boosted with DCova (1  $\times$  10<sup>6</sup> cells/mouse). Four days after the boost, OVA-specific CTL responses were analyzed by flow cytometry. In addition, we also established a more stringent model of chronic infection by i.v. injecting B6 mice with anti-CD4 antibody (300  $\mu$ g/mouse) to deplete CD4<sup>+</sup> helper T (Th) cells, followed by i.v. infection with AdVova 1 day after antibody treatment for the



assessment of the conversion effect of OVA-TEXO vaccination on CTL exhaustion, in which 'helpless' CD8<sup>+</sup> T cells demonstrated stronger functional defects.<sup>36</sup>

### Cytotoxicity assay

The *in vivo* cytotoxicity assay was performed in immunized mice with transfer of both OVAI-pulsed CFSE (3.0 μM CFSE<sup>high</sup>)-labeled (H) and control irrelevant Mut1-pulsed CFSE (0.6 μM CFSE<sup>low</sup>)-labeled (L) target splenocytes at a ratio of 1:1 (each 4 × 10<sup>6</sup> cells), as previously described.<sup>22</sup> Sixteen hours after the cell transfer, the residual CFSE<sup>high</sup> (H) and CFSE<sup>low</sup> (L) target cells remaining in the recipients' spleens were analyzed by flow cytometry.<sup>23</sup>

### RNA array analysis

Naive CD8<sup>+</sup> T cells from naive or chronically infected WT B6 mice spleens were purified using an EasySep Mouse CD8<sup>+</sup> T-Cell Isolation Kit (StemCell Technologies, Vancouver, BC, Canada), followed by Biotin-CD45RA (BD Biosciences) and MACS anti-biotin microbeads (Miltenyi Biotech). RNA isolation was performed using an RNeasy Plus Mini Kit (Qiagen Inc., Toronto, ON, Canada), cDNA was synthesized immediately using an RT<sup>2</sup> First Strand Kit (Qiagen Inc.). A panel of primers specific for T-cell anergy-associated genes (Ikarcos, Grail, Casp3, EGR2, Grg4 and Itch) was synthesized.<sup>37</sup> Real-time PCR was carried out with RT<sup>2</sup> SYBR Green qPCR Mastermix (Qiagen) using a StepOnePlus Real-time PCR system (Applied Biosystems, Burlington, ON, Canada).<sup>38</sup> The expression of each gene was normalized to β-actin. The fold induction represents the ratio of mRNA expression in CD8<sup>+</sup> T cells from chronically AdV-infected mouse spleens to that in naive mice spleens.

### Western blot analysis

Cell lysates (10 μg/lane) were loaded onto 12% acrylamide gels, subjected to sodium dodecyl sulfate-poly-acrylamide gel electrophoresis (SDS-PAGE), and subsequently transferred onto a nitrocellulose membrane (Millipore, Bedford, MA, USA). The membrane was blocked by incubation for 2 h at room temperature with ODYSSEY blocking buffer (LI-COR Bioscience, Lincoln, NE, USA) and immunoblotted with Abs specific for GRAIL and ITCH at 4 °C overnight. After three washes with PBS containing 0.05% (V/V) Tween 20, the membrane was further incubated with goat anti-rabbit IRDye800CW and scanned using an ODYSSEY instrument according to the manufacturer's instructions (LI-COR Bioscience).<sup>38</sup>

### Flow cytometric analysis

To assess the counteraction of naive CD8<sup>+</sup> T-cell anergy by OVA-TEXO, B6 mice (4–6 per group) were *i.v.* infected with AdV<sub>Gal</sub> (1 × 10<sup>8</sup> p.f.u./mouse) and 2 months later were further *i.v.* immunized with DCova and OVA-TEXO cells (1 × 10<sup>6</sup> cells/mouse). Six days after the immunization, mouse blood samples were stained with FITC-CD8 Ab and PE-tetramer, and OVA-specific CTL responses were analyzed by flow cytometry.<sup>39</sup>

To assess CTL recall responses, the vaccinated mice were then *i.v.* boosted with rLmOVA (1000 c.f.u.) 30 days after immunization and measured for OVA-specific CTL responses 4 days following the boost by flow cytometry.<sup>39</sup> To assess the molecular mechanism for OVA-TEXO-mediated counteraction of anergy, B6 mice (4–6 per group) with AdV<sub>Gal</sub>-induced chronic infection were *i.v.* immunized with OVA-TEXO cells; OVA-TEXO cells lacking IL-2, TNF-α and CD40L (2 × 10<sup>6</sup> cells/mouse); or OVA-TEXO plus anti-CD40L antibody (200 μg/mouse). The OVA-specific CTL responses in the immunized mice were assessed 6 days after immunization by flow cytometry.

### T-cell proliferation assays

In the *in vitro* T-cell proliferation assay, naive CD8<sup>+</sup> T cells purified from the splenocytes of AdV<sub>Gal</sub>- and AdVova-infected B6 mice using biotin-anti-CD45RA antibody and MACS anti-biotin microbeads (Miltenyi Biotech) followed by an EasySep Mouse CD8<sup>+</sup> T-Cell Isolation Kit (StemCell Technologies) were labeled with CFSE (3 mM). CFSE-labeled T cells were then incubated with CD3/CD28 microbeads in the presence of IL-2 (40 U/ml) and beta-mercaptoethanol (2-ME; 50 μM). Three days after incubation, the active CD8<sup>+</sup> T cells were harvested and analyzed for the determination of the number of CFSE-labeled T-cell divisions by flow cytometry. In one *in vivo* T-cell proliferation assay, naive CD8<sup>+</sup> T cells were purified from naive OTI mice or OTI mice chronically infected with AdV<sub>Gal</sub> labeled with CFSE (4 μM), and adoptively transferred (1 × 10<sup>6</sup>/mouse) into naive B6 recipients. The DCova or OVA-TEXO vaccine was injected on the following day to activate the CFSE-labeled OTI-CD8<sup>+</sup> T cells *in vivo*. Seventy-two hours later, the splenocytes were collected and analyzed by flow cytometry. In another *in vivo* T-cell proliferation assay, exhausted mCTLs purified from chronically AdVova-infected mice using PE-tetramer and MACS anti-PE-microbeads (Miltenyi Biotech) were cultured in culture medium with or without rapamycin (100 nM) for 6 h<sup>40</sup> and transferred into mice with AdV<sub>Gal</sub>-induced chronic infection, followed by OVA-TEXO (1 × 10<sup>6</sup>) vaccination. Four days after vaccination, the OVA-specific CTL responses were assessed by flow cytometry.

### Conversion of CTL exhaustion by the OVA-TEXO vaccine

To assess the conversion of mCTL exhaustion, chronically AdVova-infected B6 mice (8 per group) with CTL exhaustion were given *i.v.* OVA-TEXO cells (1 × 10<sup>6</sup> cells/mouse) or OVA-TEXO (CD40L<sup>-/-</sup>) cells, with defective CD40L (1 × 10<sup>6</sup> cells/mouse), 45–50 days after infection. To determine whether the OVA-TEXO-induced conversion of CTL exhaustion in chronic infection was dependent on DCs and CD4<sup>+</sup> T-cell help, we repeated the above experiments using OVA-TEXO vaccination of AdVova-infected DTR-CD11c mice, who received *i.p.* diphtheria toxin (DT) (300 ng/mouse) treatment once every other day starting 3 days before vaccination to deplete CD11c<sup>+</sup> DCs for a total of three times, or AdVova-infected WT B6 mice who received a single *i.p.* treatment with



anti-CD4 antibody (500 µg/mouse) 1 day before vaccination to deplete CD4<sup>+</sup> T cells.<sup>41</sup> Four days after vaccination, the mouse blood samples were collected, stained with FITC-CD8 Ab and PE-tetramer, and analyzed by flow cytometry. To assess OVA-specific CTLs in the spleens and lungs, mouse splenocytes and lung cell suspensions prepared by mincing lung tissues into small fragments and digesting them with collagenase D (1 mg/ml, Worthington Biochemical, Freehold, NJ, USA) at 37 °C for 30 min<sup>42</sup> were stained with FITC-CD8 Ab and PE-tetramer and analyzed by flow cytometry. For intracellular staining, mouse splenocytes were first incubated with FcR-blocking anti-16/32 Ab (eBioscience) for 30 min on ice to eliminate any nonspecific staining. The cells were then stained with FITC-CD8 Ab and PE-tetramer, followed by fixation and permeabilization with Cytofix/Cytoperm (BD Biosciences) according to the manufacturer's instructions. The cells were further stained with PE/Cy5-antibodies specific for various molecules, and the intracellular expression of these molecules was assessed by flow cytometry. For the intracellular staining of IFN-γ, the mouse splenocytes were first incubated in culture medium containing OVAI peptide (2 µg/ml) and Golgi-stop (0.7 µg/ml) (BD Biosciences) at 37 °C for 5 h, followed by incubation with an FcR-blocking anti-16/32 Ab for 30 min on ice. The cells were then stained with FITC-CD8 Ab and PE-tetramer, followed by fixation and permeabilization with Cytofix/Cytoperm (BD Biosciences). Intracellular staining for IFN-γ was conducted using PE/Cy5-anti-IFN-γ Ab, and the intracellular expression of IFN-γ was assessed by flow cytometry. Sample data were acquired on a FACSCalibur (BD Bioscience) and analyzed with FlowJo software (TreeStar, San Diego, CA, USA).

### Animal studies

To assess the functional effect of mCTLs in chronic infection, splenocytes from chronically AdVova- or rLmOVA-infected B6 mice 45–50 days after infection were transferred into naive B6 mice, and the recipient mice (8 per group) were injected with  $0.5 \times 10^6$  BL6-10<sub>OVA</sub> cells on the following day. The mice were killed 3 weeks after tumor cell challenge, and the lung metastatic tumor colonies were counted in a blind fashion. To examine the protective antitumor immunity conferred by the Gag-Texo vaccine, B6 mice (8/group) with AdVova-induced chronic infection were i.v. injected with Gag-Texo or DC<sub>Gag</sub> cells ( $2 \times 10^6$  cells/mouse). The immunized mice were i.v. challenged with  $0.5 \times 10^6$  BL6-10<sub>Gag</sub> cells 6 days subsequent to the immunization. To examine the therapeutic antitumor immunity conferred by the Gag-Texo vaccine, chronically infected B6 mice (8 per group) were first i.v. injected with  $0.5 \times 10^6$  BL6-10<sub>Gag</sub> cells. Three days after the tumor cell inoculation, the B6 mice were then i.v. injected with Gag-Texo or DC<sub>Gag</sub> cells ( $1 \times 10^6$  cells/mouse). The mice were killed 3 weeks after tumor cell challenge, and the lung metastatic tumor colonies were counted by an individual blinded to the study conditions. Metastases on freshly isolated lungs appeared as discrete black-pigmented foci that were easily distinguishable

from normal lung tissues and confirmed by histological examination. Metastatic foci too numerous to count were assigned an arbitrary value of  $> 300$ .<sup>24</sup>

### Statistical analyses

Unless stated otherwise, the data are expressed as the mean (with s.d.). Statistical analyses were performed using the Mann–Whitney *U*-test for the comparison of variables from different groups in animal studies or Student's *t*-test for the comparison of variables from different groups in all other studies. Probability values of  $P > 0.05$ ,  $P < 0.05$  and  $P < 0.01$  are considered statistically not significant, significant and very significant, respectively.<sup>39</sup>

## RESULTS

### OVA-expressing adenoviral vector induces chronic infection in mice

Distinctive CD8<sup>+</sup> T-cell responses ranging from immunogenic CTL responses to CTL exhaustion or depletion have been reported to be elicited post vaccination with adenoviral vectors (AdVs) expressing different antigens, at various doses, or through different routes.<sup>31,43–48</sup> For example, the persistence of adenoviral transgene expression in AdV-infected mice led to CTL inflation,<sup>46</sup> and mice i.v. infected with β-galactosidase (Gal)-expressing AdV<sub>Gal</sub> developed a chronic infection with CTL exhaustion and deletion.<sup>31</sup> Unfortunately, the Gal-specific PE tetramer, which is useful for detecting Gal-specific CTLs, is not commercially available, which makes it difficult to study chronic infection in this model. To assess whether a replication-deficient transgene, OVA-expressing AdVova,<sup>33</sup> induces chronic infection in mice, C57BL/6 (B6) mice were i.v. infected with AdVova. Our analysis demonstrated that 60 days later, AdVova infection resulted in a dose-dependent (Supplementary Figure 1) OVA-specific memory CD8<sup>+</sup> T-cell expansion (Figure 1a). The expanded mCTLs had decreased cell surface T-cell memory markers, CD62L and IL-7R, when compared with mCTLs developed in rLmOVA-immunized mice (Figure 1b). Interestingly, we found that these mCTLs expressed cell surface CD40 (Figure 1b). Importantly, we also found that these mCTLs upregulated inhibitory molecules, such as PD-1, PD-L1 and LAG-3 (Figure 1b), indicating that these mCTLs may be exhausted. To assess the functional traits of these potentially exhausted CTLs, including their capacity for Ag-specific cell killing and CTL recall responses, we performed flow cytometric analyses to measure cellular IFN-γ expression, cytolytic effectiveness and CTL recall responses following antigen boost and also conducted animal studies to analyze protective immunity against OVA-expressing tumor (BL6-10<sub>OVA</sub>) challenge. We determined that only 17% (1.37% vs 8.11%) of these CTLs possessed intracellular IFN-γ in comparison to nearly 75% (5.16/7.06) of IFN-γ-positive CTLs observed in rLmOVA-immunized controls (Figure 1c). This observation clearly indicates that CTLs display a significant reduction in the expression of an effector cytokine, IFN-γ, during chronic infection. In addition, these CTLs also showed defects in the cytolytic response against OVA-specific, highly

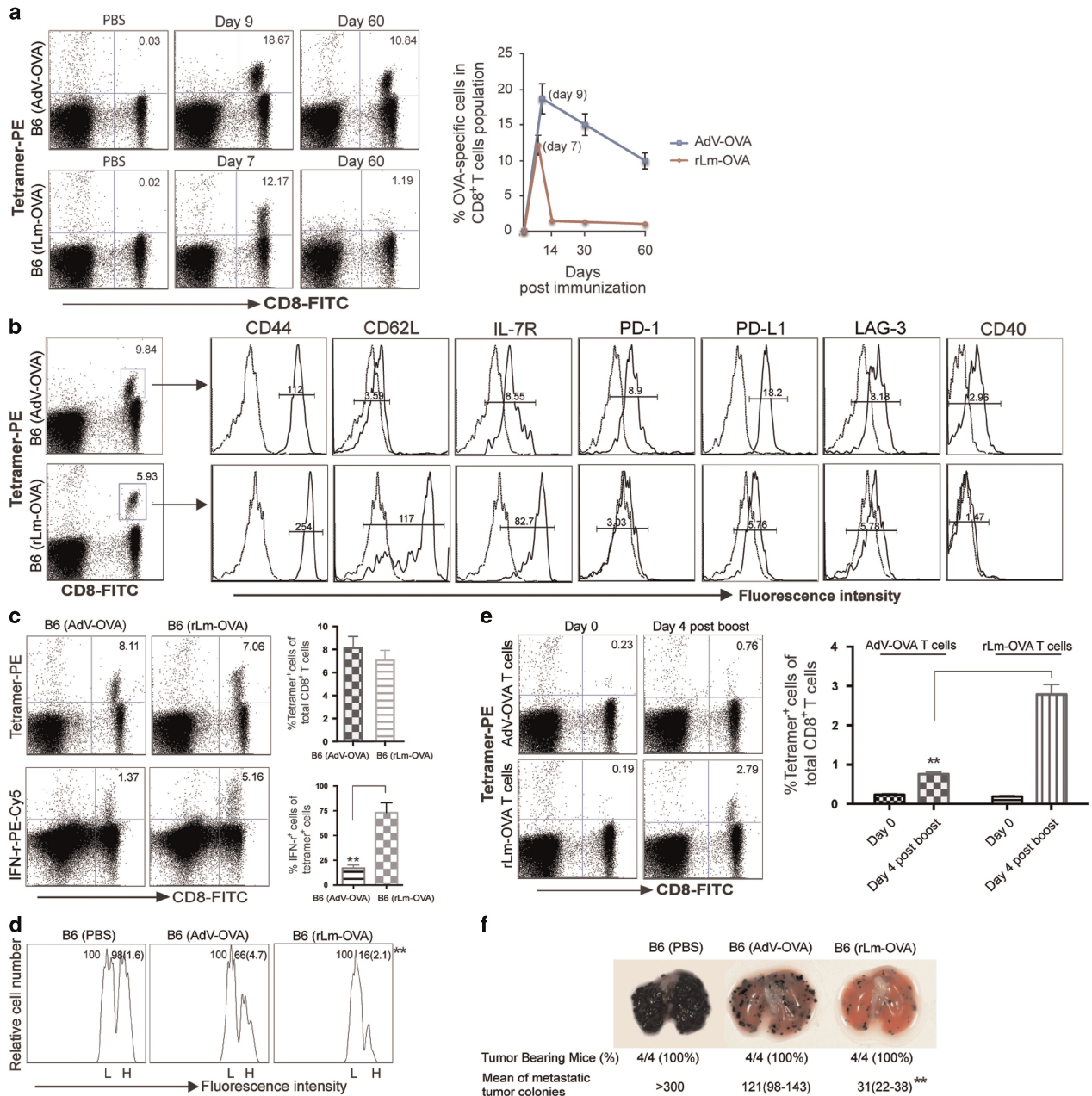


**Figure 1** AdVova induces chronic infection in mice. **(a)** OVA-specific CTL responses were analyzed at the indicated days post-AdVova or rLmOVA infection by flow cytometry. The value in each panel represents the percentage of OVA-specific (tetramer-positive) CD8<sup>+</sup> T cells in the total CD8<sup>+</sup> T-cell population. **(b, c)** To enhance mCTLs in rLmOVA-infected mice, C57BL/6 mice were first transferred with  $1 \times 10^4$  naive CD4<sup>+</sup> OTII and  $1 \times 10^4$  naive OTI CD8<sup>+</sup> T cells to increase the numbers of precursor T cells before rLmOVA infection. Sixty days after the infection, we performed flow cytometric analyses. **(b)** CD8<sup>+</sup> T cells with positive PE-tetramer and FITC-CD8 staining were gated (rectangle) for further assessment of the expression of the indicated molecules (solid lines on the right). Mean fluorescence intensity (MFI) numbers are indicated in each panel. Dotted lines (on the left) represent isotype-matched controls. The control MFI numbers for the upper and lower panels were 2.16 and 3.28, respectively. **(c)** CD8<sup>+</sup> T cells were permeabilized for the assessment of intracellular IFN- $\gamma$  by flow cytometry. The value in each panel represents the percentage of CD8<sup>+</sup> T cells producing IFN- $\gamma$  in the total CD8<sup>+</sup> T-cell population. **(d)** *In vivo* cytotoxicity assay. Sixty days after the infection, we performed an *in vivo* cytotoxicity assay as described in Materials and methods. The value in each panel represents the percentage of CFSE<sup>high</sup> vs CFSE<sup>low</sup> target cells remaining in the spleen. **(e, f)** Sixty days after the infection, splenocytes from AdVova-infected mice were adoptively transferred into C57BL/6 mice, and 1 day after transfer, the mice had 0.23% OVA-specific mCTLs, similar to the 0.19% OVA-specific mCTLs in rLmOVA-infected mice. **(e)** These mice were boosted with DCova. Four days after the boost, their peripheral blood samples were analyzed for OVA-specific memory CTL recall responses using flow cytometry. The value in each panel represents the percentage of PE-tetramer-positive CD8<sup>+</sup> T cells in the total CD8<sup>+</sup> T-cell population. **(f)** The mice were i.v. injected with BL6-10<sub>OVA</sub> tumor cells and were killed 3 weeks later. The numbers of lung metastatic tumor colonies were counted. \* $P < 0.05$ , \*\* $P < 0.01$ . Error bars represent s.d. One representative experiment of two to three is shown.

CFSE-labeled (H) target cells (Figure 1d) in mCTL recall responses upon DC<sub>OVA</sub> boost (Figure 1e) and in their immune response to OVA-expressing BL6-10<sub>OVA</sub> tumors (Figure 1f), indicating that these OVA-specific mCTLs are indeed functionally exhausted in an AdVova-induced chronic infection model. Taken together, our observations suggest that AdVova-infected mice represent a new chronic infection mouse model with mCTL inflation and exhaustion. In addition, we also assessed mCTLs in AdV<sub>Gal</sub>-infected mice using mouse peripheral blood samples stained with antibodies for CD8 and CD44 (memory T-cell marker). We demonstrated that these CD8<sup>+</sup>CD44<sup>+</sup> mCTLs also expressed inhibitory PD-1 and PD-L1 (Supplementary Figure 2), confirming that AdV<sub>Gal</sub>-infected mice also represent a chronic infection animal model useful for assessing the immunogenicity of our OVA-*Texo* vaccine.

### CD8<sup>+</sup> T-cell anergy in chronic infection

A bystander chronic infection associated with some level of immune tolerance often enhances the susceptibility of chronically infected hosts to a variety of co-infections.<sup>49</sup> However, the underlying mechanism is not clear. To assess potential immune tolerance in our chronic infection model, we examined OVA-specific CTL responses derived following vaccination with DC<sub>OVA</sub> in wild-type (WT) B6 and chronically AdV<sub>Gal</sub>-infected B6 mice. This analysis revealed that DC<sub>OVA</sub> induced ~3-fold (0.62% vs 2.24%) less OVA-specific CTL priming at day 6 post immunization and ~9-fold (2.24% vs 21.79%) less mCTL recall responses measured at day 4 after the boost in mice with chronic infection (Figure 2Ac and d), compared with the responses observed in WT B6 mice (Figure 2Aa and b). These data indicate that some immune tolerance occurs in the presence of the AdV<sub>Gal</sub>-induced chronic infection. To assess whether the immune tolerance involves CD8<sup>+</sup> T cells, we performed an *in vitro* T-cell proliferation assay. In the assay, naive CD8<sup>+</sup> T cells purified from chronically infected B6 mice or WT B6 mice were labeled with CFSE and activated with anti-CD3/CD28 beads and IL-2 *in vitro*. Three days later, these T cells were analyzed by flow cytometry. Naive CD8<sup>+</sup> T cells derived from chronically AdVova-infected B6 mice underwent less cell division (78.3%) (Figure 2Bc) than those (95.2%) from WT B6 mice (Figure 2Bb), indicating that naive CD8<sup>+</sup> T cells are anergic during chronic infection. Similar data were also observed in naive CD8<sup>+</sup> T cells labeled with CFSE and stimulated with CD3/28 beads and IL-2 in chronically AdV<sub>Gal</sub>-infected B6 mice (Supplementary Figure 3a). In addition, we also performed an *in vivo* T-cell proliferation assay. In the assay, naive CD8<sup>+</sup> T cells purified from OTI mice or AdV<sub>Gal</sub>-infected OTI mice were labeled with CFSE and transferred into WT B6 mice. One day after the transfer, the mice were immunized with DC<sub>OVA</sub>, and the mouse splenocytes were analyzed 3 days later by flow cytometry. This experiment demonstrated that CFSE-labeled OTI CD8<sup>+</sup> T cells derived from AdV<sub>Gal</sub>-infected OTI mice underwent fewer cell divisions (72.7%) (Figure 2Ce) than those (95.2%) derived from uninfected OTI mice (Figure 2Cb), thus confirming that naive

CD8<sup>+</sup> T cells with a chronic infection background are indeed anergic. It has been shown that naive splenocytes containing B and T cells and DCs upregulated inhibitory PD-L1 in the course of chronic infection, but the subset of immune cells expressing PD-L1 was not defined.<sup>36</sup> To assess the phenotype of anergic naive CD8<sup>+</sup> T cells in our AdVova-induced chronic infection animal model, we performed flow cytometric analysis. Interestingly, we found that naive CD45RA<sup>+</sup>CD8<sup>+</sup> T cells<sup>50</sup> in B6 mice with AdVova-induced chronic infection had increased inhibitory PD-L1 and BTLA molecules compared with cells derived from uninfected naive B6 mice (Figure 2D). In support of this, we found that naive CD8<sup>+</sup> T cells in AdV<sub>Gal</sub>-induced chronic infection also upregulated inhibitory PD-L1, BTLA, B7H3 and LAG3 (Supplementary Figure 3b). Interestingly, we demonstrated that ~44% of the naive CD8<sup>+</sup> T cells in chronic infection, but not in healthy naive B6 mice, expressed cell surface CD40 (Figure 2D). In addition, we also performed RT-PCR analysis to assess the expression of T-cell anergy-associated genes and showed that the naive CD8<sup>+</sup> T cells in an AdVova-induced chronic infection model upregulated the T-cell anergy-associated genes *Grail* and *Itch* (Figure 2E), which implies that CD8<sup>+</sup> T-cell tolerance in chronic infection is associated with naive CD8<sup>+</sup> T-cell anergy. This was further confirmed by western blotting analysis, demonstrating the upregulation of the *Grail* and *Itch* molecules at the protein level in naive CD8<sup>+</sup> T cells derived from mice with AdVova- and AdV<sub>Gal</sub>-induced chronic infection (Figure 2F, Supplementary Figure 3c).

### OVA-*Texo* counteracts naive CD8<sup>+</sup> T-cell anergy in chronic infection

To evaluate whether the OVA-*Texo* vaccine counteracts the immune tolerance in our chronic infection model, we assessed OVA-specific CTL responses derived from OVA-*Texo* vaccination of WT B6 and chronically AdV<sub>Gal</sub>-infected B6 mice. In contrast to significantly decreased OVA-specific CTL responses in DC<sub>OVA</sub>-vaccinated mice with chronic infection, relatively smaller, but still comparable, CTL priming (1.67%) and mCTL recall (11.91%) responses were found in OVA-*Texo*-immunized mice with chronic infection (Figure 2Ag and h) when compared with those in WT B6 mice (2.78 and 18.70%) (Figure 2Ae and f). In contrast to the significant reduction of DC<sub>OVA</sub>-induced CTL priming and recall responses in mice with chronic infection, OVA-*Texo* stimulated comparable CTL priming and recall responses in mice with chronic infection compared with WT mice, indicating that the OVA-*Texo* vaccine can counteract T-cell tolerance caused by chronic infection. Interestingly, the OVA-*Texo* vaccine was also found to induce comparable proliferation (94.4%) of CFSE-labeled CD8<sup>+</sup> T cells transferred from AdV<sub>Gal</sub>-infected OTI mice (Figure 2Cf) compared with that (92.3%) of CFSE-labeled CD8<sup>+</sup> T cells transferred from WT OTI mice (Figure 2Cc). Our data thus indicate that the OVA-*Texo* vaccine is capable of counteracting naive CD8<sup>+</sup> T-cell anergy in chronic infection.



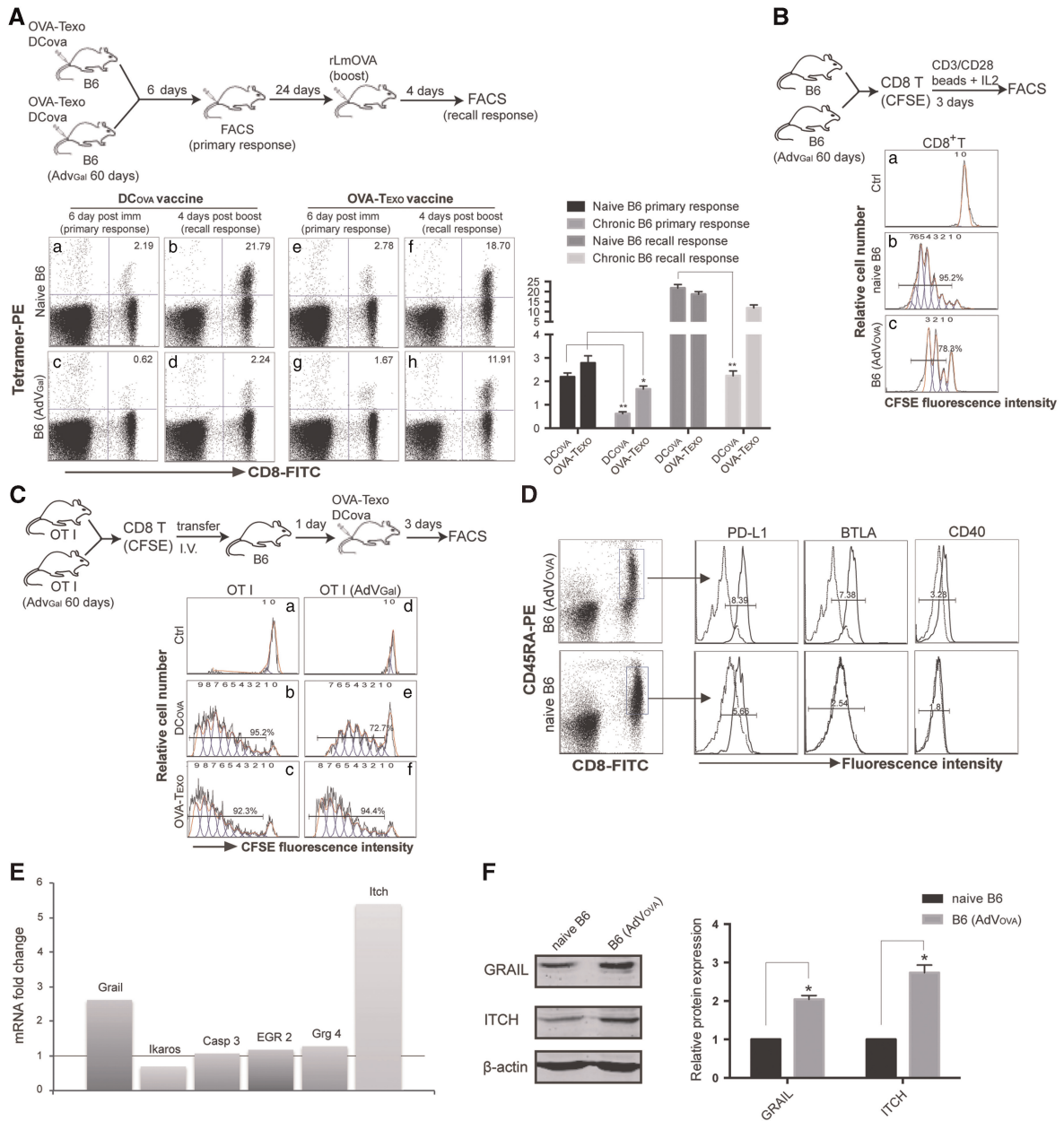


**Figure 2** T-cell energy in chronic infection. **(A)** We assessed CTL priming and recall responses as described in the diagram. The value in each panel represents the percentage of OVA-specific (tetramer-positive) CD8<sup>+</sup> T cells in the total CD8<sup>+</sup> T-cell population. **(B, C)** We assessed cell proliferation as described in the diagrams. Cell divisions were monitored by analyzing CFSE dilution. Histograms show the FACS profiles of **(B)** CD8<sup>+</sup>/CFSE<sup>+</sup> T cells from the *in vitro* proliferation assay or **(C)** PE-tetramer<sup>+</sup>/CFSE<sup>+</sup> T cells from the *in vivo* proliferation assay. The numbers of cell divisions were indicated on top of each panel, and the percentages of dividing cells were indicated on top of the number of divisions. **(D)** Peripheral blood samples from naive mice or chronically AdVova-infected mice were stained with PE-CD45RA, FITC-CD8 and PE-Cy5-labeled Abs and then analyzed by flow cytometry. Naive CD8<sup>+</sup> T cells with positive PE-CD45RA and FITC-CD8 staining were gated (rectangle) for further measurement of the expression of co-stimulatory or inhibitory molecules (solid lines on the right). Mean fluorescence intensity (MFI) numbers are indicated in each panel. Dotted lines (on the left) represent isotype-matched controls. The control MFI numbers for the upper panel's PD-L1/BTLA and CD40 were 1.28 and 1.80, respectively, while the control MFI numbers for the lower panel's PD-L1/BTLA and CD40 were 2.51 and 1.80, respectively. **(E)** The expression of anergy-associated genes was assessed by RT-PCR using mRNA purified from naive CD8<sup>+</sup> T cells derived from naive or chronically infected mouse splenocytes. The numbers of mRNA fold changes (the ratio of mRNA expression of each gene in naive CD8<sup>+</sup> T cells derived from AdVova-infected mice vs WT B6 mice) are indicated. **(F)** Western blotting analysis. The protein extracts were analyzed by western blotting. Each protein band intensity was quantitated using a computational densitometer in the ODYSSEY software. The expression ratio (ER) represents the protein expression of each gene normalized to the matching  $\beta$ -actin control. The relative protein expression (RPE) represents the ratio of the ER of each gene in AdVova-infected B6 mice vs that in naive B6 mice. \* $P < 0.05$ , \*\* $P < 0.01$ . Error bars represent the s.d. One representative experiment of two to three is shown.

### OVA-Texo-induced counteraction of CD8<sup>+</sup> T-cell anergy depends upon CD40L signaling

It has been demonstrated that the cytokines IL-2 and TNF- $\alpha$  along with CD40L co-stimulation counteract T-cell anergy or tolerance.<sup>51–53</sup> To assess a potential molecular mechanism for the OVA-Texo-mediated counteraction of CD8<sup>+</sup> T-cell anergy, we generated a panel of OVA-Texo vaccines with various molecular defects, such as OVA-Texo(IL-2<sup>-/-</sup>), OVA-Texo(TNF- $\alpha$ <sup>-/-</sup>) and OVA-Texo(CD40L<sup>-/-</sup>), lacking the expression of IL-2, TNF- $\alpha$  and CD40L, respectively. Mice with AdV<sub>Gal</sub>-induced chronic infection were individually immunized with each of these vaccines, and their OVA-specific CTL responses were assessed by flow cytometry on day 6 after immunization. This approach demonstrated that CD40L deficiency alone reduced OVA-Texo-stimulated OVA-specific CTL responses during chronic infection by 85%, though the CTL responses were also significantly downregulated when using the OVA-Texo(TNF- $\alpha$ <sup>-/-</sup>) and OVA-Texo(IL-2<sup>-/-</sup>) vaccines (Figure 3a). Our data indicate that the OVA-Texo-induced counteraction of CD8<sup>+</sup> T-cell anergy in chronic infection is mainly mediated by CD40L signaling. In addition, a blockade of CD40L using an antagonistic anti-CD40L antibody also significantly inhibited OVA-Texo-stimulated CTL responses in mice with chronic infection (Figure 3b), thus confirming the above observation. Taken together, our data determine that the OVA-Texo vaccine is capable of counteracting naïve CD40-expressing CD8<sup>+</sup> T-cell anergy/tolerance in chronic infection via signaling through CD40L.

### The OVA-Texo vaccine converts CTL exhaustion in chronic infection

In our further experiments, we examined whether the OVA-Texo vaccine would enhance the responses of functionally exhausted CD8<sup>+</sup> T cells in mice with AdVova-induced chronic infection. This is a more stringent model of chronic infection because the primary infection with AdVova is performed in the absence of CD4<sup>+</sup> T cells, which are initially eliminated using an anti-CD4 Ab. The exhausted CTLs derived from ‘helpless’ CD8<sup>+</sup> T cells in the T-cell priming phase of the infection have stronger functional defects in IFN- $\gamma$  production and cytotoxicity.<sup>54</sup> Mice with AdVova-induced chronic infection were boosted with the OVA-Texo vaccine. Four days after the boost and the cell number increased, IFN- $\gamma$  expression and cytolytic activity of OVA-specific CTLs were analyzed by flow cytometry. These experiments demonstrated that there were ~4-fold (10.85% vs 2.70%) more of OVA-specific CTLs in OVA-Texo-boosted mouse peripheral blood at day 4 after the boost (Figure 4a), indicating that the OVA-Texo vaccine can directly convert CTL exhaustion. The 4-fold increase in OVA-specific CTLs was likely generated from the previously exhausted mCTLs because the primary OVA-specific CTLs derived from the OVA-Texo boost did not occur in the peripheral blood at day 4, but peaked at day 6 post stimulation (Supplementary Figure 4). To further confirm this, we transferred exhausted mCTLs derived from chronically AdVova-infected B6 (CD45.2<sup>+</sup>) mice into chronically AdV<sub>Gal</sub>-

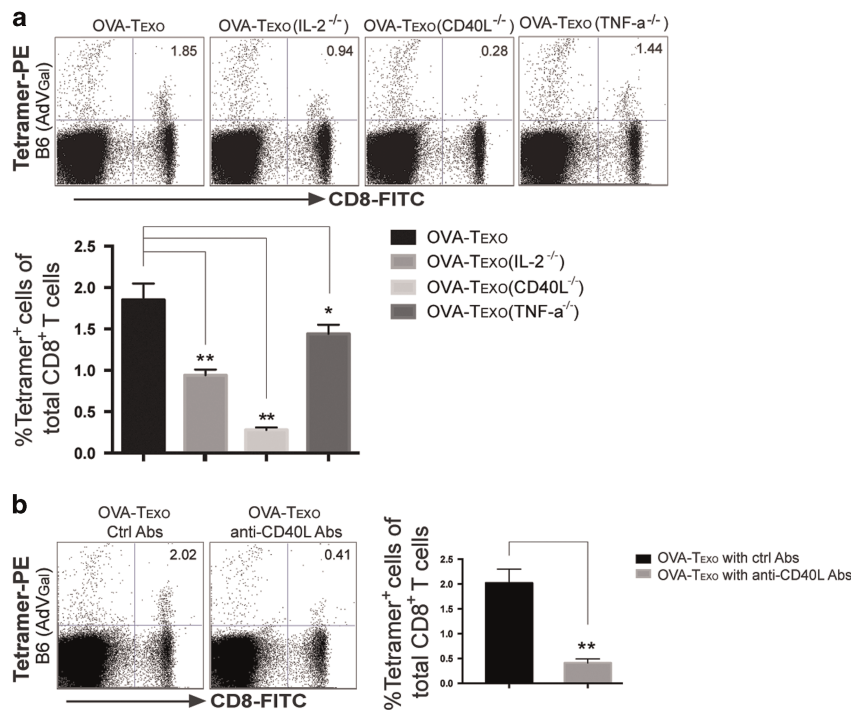


**Figure 3** OVA-Texo counteracts CD8<sup>+</sup> T-cell anergy via CD40L signaling. AdV<sub>Gal</sub>-infected C57BL/6 mice were immunized with (a) the OVA-Texo vaccine or the OVA-Texo vaccine deficient for one of several molecules or (b) the OVA-Texo vaccine plus anti-CD40L antibody treatment. Six days after the immunization, mouse peripheral blood samples were stained with PE-tetramer and FITC-CD8, and analyzed for the assessment of OVA-specific CTLs by flow cytometry. The value in each panel represents the percentage of PE-tetramer-positive CD8<sup>+</sup> T cells in the total peripheral CD8<sup>+</sup> T-cell population. \**P*<0.05, \*\**P*<0.01. Error bars represent the s.d. One representative experiment of two is shown.

infected B6.1 (CD45.1<sup>+</sup>) mice and performed a OVA-Texo boost. As expected, all OVA-specific CTLs with an ~4-fold increase at day 4 post boost exclusively expressed CD45.2, but not CD45.1 (Figure 4b), thus confirming that this increased cell population represents the OVA-Texo-induced expansion of exhausted CD45.2<sup>+</sup> mCTLs. Our data thus suggest that the OVA-Texo vaccine is capable of efficiently converting CTL exhaustion in chronic infection by significantly increasing the number of previously exhausted CTLs. In addition to the CTL increase in the peripheral blood, there were also ~4-fold more OVA-specific CTLs in the spleens and lungs following the boost (Figure 4c). Consistent with a previous report,<sup>36</sup> no significant change in the expression of inhibitory molecules (PD-1, PD-L1 and LAG3) could be observed on CTLs after the OVA-Texo boost (Figure 4a). We next measured the OVA-Texo-induced expression of an effector cytokine, IFN- $\gamma$ , in exhausted CTLs on a 'per-cell' basis by intracellular staining of IFN- $\gamma$ . We observed that 88% of the OVA-specific CTLs were IFN- $\gamma$ <sup>+</sup> in OVA-Texo-treated mice, compared with only ~20% of IFN- $\gamma$ -producing OVA-specific CTLs in PBS control mice (Figure 4d). In addition, we also used flow cytometry to measure the intracellular level of a useful marker for memory T-cell activation and functionality, diacetylated histone-H3 (diAcH3).<sup>55</sup> Our experiments revealed that OVA-Texo-stimulated, OVA-specific CTLs had increased diAcH3 levels (Figure 4a). Because in chronic infection, exhausted CTLs have a functional defect in their ability to lyse target cells (Figure 1d),<sup>11</sup> we attempted to determine whether OVA-Texo-converted CTLs had restored cytolytic effectiveness. To achieve this, we performed an *in vivo* cytotoxicity assay by transferring highly and lowly CFSE-labeled OVA-specific (H) and non-specific (L) target cells in a 1:1 ratio into OVA-Texo-immunized mice and monitoring the lysis of OVA-specific (H) target cells by flow cytometry. The results showed a significant increase in OVA-specific cytolytic responses (93.5% lysis) in OVA-Texo-treated mice compared with weak target cell lysis (13.5%) in untreated mice (Figure 4e). Taken together, our data indicate that the OVA-Texo vaccine efficiently converts CTL exhaustion by not only increasing the number of CTLs but also restoring their function.

#### **OVA-Texo-induced conversion of CTL exhaustion is relatively independent of host CD4<sup>+</sup> T cells and completely independent of host DCs**

We showed previously that our OVA-Texo vaccine stimulated OVA-specific CTL responses relatively independently of host CD4<sup>+</sup> T cells, but completely independent of host DCs in WT B6 mice.<sup>23</sup> To assess whether the OVA-Texo vaccine also converts CD4<sup>+</sup> T/DC-independent CTL exhaustion in chronic infection, we repeated our experiments in AdVova-infected B6 mice in the presence of anti-CD4 antibody treatment to deplete CD4<sup>+</sup> T cells or in AdVova-infected transgenic DTR-CD11c mice treated with diphtheria toxin (DT) to deplete CD11c<sup>+</sup> DCs, as we previously described.<sup>41</sup> We determined that the OVA-Texo vaccine stimulated slightly less CTL responses (6.0%) in anti-CD4 antibody-treated C57BL/6, but similar

CTL responses (8.3%) in DT-treated DTR-CD11c mice with chronic infection 4 days post vaccination, compared with CTL responses in matching control mice (7.8% and 8.2%, respectively; Figure 4f). These data indicate that our OVA-Texo vaccine is capable of directly converting CTL exhaustion in the absence of CD4<sup>+</sup> T cells and DCs in chronic infection.

#### **OVA-Texo-induced conversion of CTL exhaustion depends upon CD40L signaling**

Because CD40L signaling by the OVA-Texo vaccine was found to be important for the counteraction of CD8<sup>+</sup> T-cell tolerance, we wanted to examine whether CD40L has a role in the conversion of CTL exhaustion by the OVA-Texo vaccine. Chronically AdVova-infected B6 mice with CTL exhaustion were immunized with the OVA-Texo(CD40L<sup>-/-</sup>) vaccine, which lacks CD40L signaling. Interestingly, CD40L deficiency alone caused a significant decrease in the ability of the vaccine to induce T-cell proliferation; the induced proliferation went from a ~4-fold increase with OVA-Texo (2.70% vs 10.85%) down to no change with OVA-Texo(CD40L<sup>-/-</sup>) (2.87% vs 3.25%) (Figure 5a), indicating that the OVA-Texo-induced conversion of CTL exhaustion occurs mainly via CD40L signaling. We also measured the OVA-Texo stimulation-induced expression of an effector cytokine, IFN- $\gamma$ , in exhausted CTLs on a 'per-cell' basis. This revealed that 86% of the total OVA-specific CTL population produced IFN- $\gamma$  in the OVA-Texo-treated mice, compared with only 26% of the OVA-specific CD8<sup>+</sup> T cells producing IFN- $\gamma$  in the OVA-Texo(CD40L<sup>-/-</sup>)-stimulated mice (Figure 5b), which was similar to the 22% of OVA-specific CD8<sup>+</sup> T cells producing IFN- $\gamma$  in chronically infected control PBS-treated mice (Figure 4d). Our data thus indicate that CD40L signaling has a critical role in the conversion of CTL exhaustion by the OVA-Texo vaccine.

#### **OVA-Texo converts CTL exhaustion through activation of the mTORC1 pathway**

It has been shown that CD40L signaling assures T-cell activation via the mTORC1 pathway.<sup>56</sup> To assess whether the OVA-Texo vaccine activates the mTORC1 pathway, we analyzed CTLs by flow cytometry for the phosphorylation status and intracellular expression of a panel of molecules associated with the mTORC1 pathway, including Akt, mTORC1-regulated S6, eIF4E and T-bet. We determined that OVA-specific CTLs upregulated their levels of pAkt, pS6, peIF4E and T-bet as well as Ki67 (a protein associated with cell cycle progression) in chronically AdVova-infected B6 mice following OVA-Texo vaccination (Figure 5c). This indicates that the OVA-Texo vaccine stimulates the proliferation of exhausted CTLs at least in part by activating the PI3K/Akt/mTORC1 pathway. In addition, OVA-specific CTLs did not show any upregulation of mTORC1-related molecules in OVA-Texo(CD40L<sup>-/-</sup>)-stimulated mice (data not shown), suggesting that OVA-Texo converts CTL exhaustion via the CD40L-induced activation of the mTORC1 pathway. Rapamycin is a well-described inhibitor for the mTORC1 pathway.<sup>36</sup> To assess



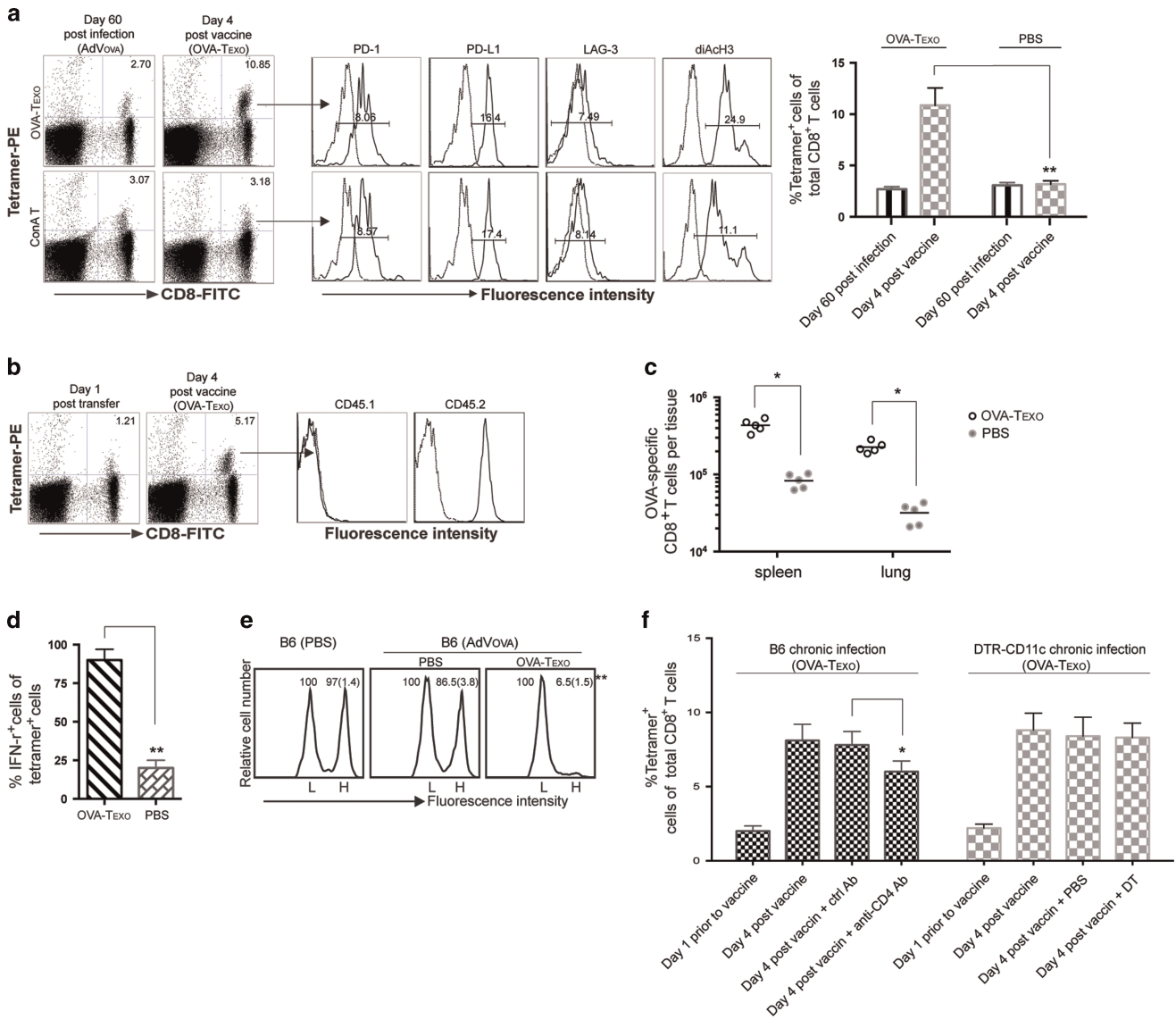


**Figure 4** The OVA-Texo vaccine converts T-cell exhaustion. **(a)** OVA-specific CTL responses were analyzed on the indicated days by flow cytometry. OVA-specific CD8<sup>+</sup> T cells with positive PE-tetramer and FITC-CD8 staining were gated (arrow) for the further assessment of PD-1, PD-L1 and diAch3 expression (solid lines on the right). The mean fluorescence intensities (MFI) are indicated. Dotted lines (on the left) represent isotype-matched controls. The value in each panel represents the percentage of PE-tetramer-positive CD8<sup>+</sup> T cells in the total CD8<sup>+</sup> T-cell population. **(b)** OVA-specific CTLs were purified from the splenocytes of chronically AdVova-infected B6 mice (CD45.2<sup>+</sup>) using PE-tetramer staining followed by anti-PE microbeads and then transferred into B6.1 (CD45.1<sup>+</sup>) mice with AdV<sub>Gal</sub>-induced chronic infection. The transferred OVA-specific CTLs in the mice were assessed by flow cytometry 1 day post transfer. The mice were also boosted with the OVA-Texo vaccine and assessed for CTL responses 4 days post boost using triple staining for PE-tetramer, FITC-CD8 and PE-Cy5-CD45.1 or CD45.2 by flow cytometry. The OVA-specific CD8<sup>+</sup> T cells with positive PE-tetramer and FITC-CD8 staining were gated (arrow) for further measurement of the expression of CD45.1 and CD45.2 (solid lines on the right). Dotted lines (on the left) represent isotype-matched antibody controls. **(c)** The total number of PE-tetramer<sup>+</sup>/FITC-CD8<sup>+</sup> T cells in the spleens and lungs following OVA-Texo immunization were analyzed by flow cytometry using splenocytes and lung tissue cell suspensions. **(d)** The percentage of IFN- $\gamma$  producing cells in the PE-tetramer<sup>+</sup>/FITC-CD8<sup>+</sup> T-cell population was also analyzed in the indicated conditions, as described in Figure 1c. **(e)** An *in vivo* cytotoxicity assay was performed in chronically AdVova-infected OVA-Texo-treated mice, as described in Figure 1d. The value in each panel represents the percentage of CFSE<sup>high</sup> vs CFSE<sup>low</sup> target cells remaining in the spleen. **(f)** AdVova-infected B6 mice with anti-CD4 antibody treatment or AdVova-infected DTR-CD11c mice with diphtheria toxin (DT) treatment were vaccinated with OVA-Texo 1 day after treatment. At day 4 following the vaccination, blood samples were collected, double stained with FITC-CD8 and PE-tetramer, and analyzed by flow cytometry. The percentages of PE-tetramer-positive CD8<sup>+</sup> T cells in the total CD8<sup>+</sup> T-cell population in anti-CD4 antibody- and DT-treated mice vs those in matching untreated control mice are indicated. \* $P < 0.05$ , \*\* $P < 0.01$ . Error bars represent the s.d. One representative experiment of two to three is shown.

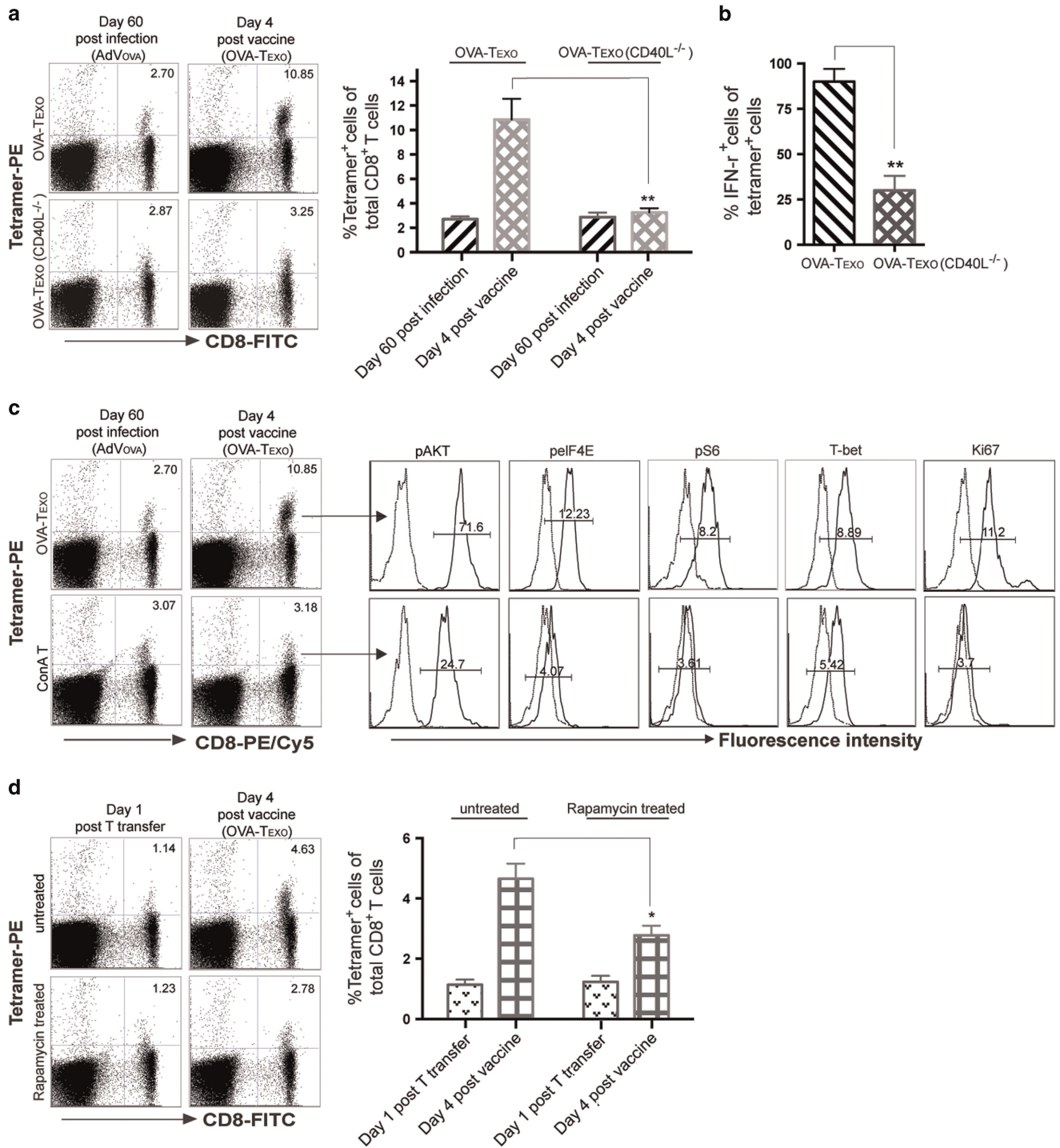


**Figure 5** The OVA-Texo vaccine converts CTL exhaustion through CD40L signaling via the mTORC1 pathway. **(a)** AdVova-infected C57BL/6 mice were immunized with OVA-Texo 60 days after primary infection. Prior to and 4 days post immunization, mouse peripheral blood was analyzed for OVA-specific CTLs by flow cytometry. The value in each panel represents the percentage of PE-tetramer-positive CD8<sup>+</sup> T cells in the total CD8<sup>+</sup> T-cell population. **(b)** The percentage of IFN- $\gamma$  producing cells in the PE-tetramer<sup>+</sup> and FITC-CD8<sup>+</sup> T-cell population was analyzed in each treatment group. **(c)** The mouse splenocytes from **(a)** were triple-stained with PE-Tetramer, FITC-CD8 and PE/Cy5-labeled Abs. The OVA-specific CD8<sup>+</sup> T cells with positive PE-tetramer and FITC-CD8 staining were gated (arrow) and assessed for the expression of pAKT, pelf4E, pS6, T-bet and Ki67 (solid lines on the right). The mean fluorescence intensity (MFI) numbers of solid lines are indicated. Dotted lines (on the left) represent isotype-matched controls. The MFI numbers of the dotted lines in the upper panels were similar to those in the lower panels. **(d)** Rapamycin-treated or untreated CTLs purified from chronically AdV<sub>Gal</sub>-induced chronic infection, followed by OVA-Texo vaccination 1 day post transfer. The OVA-specific CTLs were detected by flow cytometry. The value in each panel represents the percentage of PE-tetramer-positive CD8<sup>+</sup> T cells in the total peripheral CD8<sup>+</sup> T-cell population. \* $P < 0.05$ , \*\* $P < 0.01$ . Error bars represent the s.d. One representative experiment of two is shown.

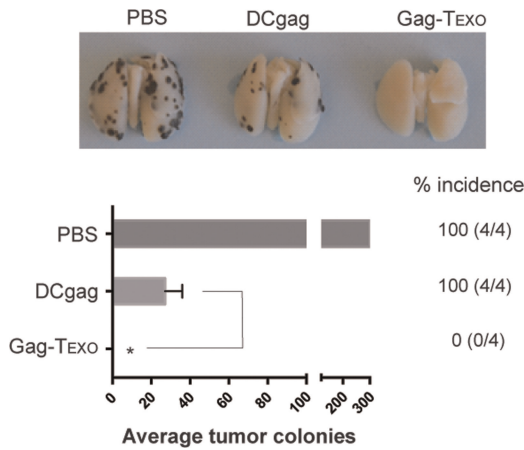


**Figure 6** Gag-TEXO vaccine induces therapeutic antitumor immunity in mice with chronic infection. AdVova-infected mice were i.v. injected with BL6-10<sub>Gag</sub> cells. Three days later, the mice were vaccinated with Gag-TEXO and DC<sub>Gag</sub>. The mice were killed 3 weeks after tumor cell challenge, and lung-metastatic tumor colonies with black color were counted in the lungs. \**P*<0.05. Error bars represent the s.d. One representative experiment of two is shown.

whether activation of the mTORC1 pathway is responsible for OVA-TEXO-induced conversion of CTL exhaustion, we treated exhausted CTLs purified from chronically infected mice with rapamycin and transferred them into chronically AdV<sub>Gal</sub>-infected B6 mice, followed by OVA-TEXO vaccination. Interestingly, rapamycin treatment significantly reduced the efficiency of the OVA-TEXO boost from the original ~4-fold (4.63% vs 1.14%) down to only ~2-fold (2.78% vs 1.23%) (Figure 5d). Our data thus confirm that OVA-TEXO directly converts CTL exhaustion either mostly or at least partly through the activation of the mTORC1 pathway.

### Gag-TEXO vaccine induces Gag-specific therapeutic immunity in a chronic infection model

To assess potential therapeutic immunity in this model, chronically AdVova-infected B6 mice were injected with Gag-expressing BL6-10<sub>Gag</sub> melanoma cells. Three days after tumor cell challenge, the chronically infected mice were immunized with the Gag-TEXO or DC<sub>Gag</sub> vaccine. Notably, we determined that Gag-TEXO, but not the DC<sub>Gag</sub> vaccine, completely eradicated all established BL6-10<sub>Gag</sub> lung metastases, even in the presence of chronic infection (Figure 6), indicating that our Gag-TEXO vaccine is capable of inducing therapeutic immunity against established Gag-expressing tumors in AdVova-induced chronic infection.

## DISCUSSION

Vaccines based on the recombinant human E1/E3-depleted adenovirus-5 (AdV-5) vector are well characterized and have been shown to be effective at inducing CD8<sup>+</sup> CTL responses due to their strong immunogenicity.<sup>57</sup> Adenoviral vectors are easy to manipulate to infect different types of cells, and their safety is well defined because the vector genome does not

integrate into the cellular DNA.<sup>58</sup> However, adenoviral transgene expression could still persist in a host at low levels for a relatively long time<sup>43,44,46</sup> and even for one year post-AdV infection.<sup>43,44</sup> Exhausted CTLs, resulting from excessive or persistent Ag stimulation, often present a significant barrier to immune responses and managing chronic infection.<sup>59</sup> For example, in the exhausted state of LCMV-infected mice, LCMV-specific CTLs become subject to multiple inhibitory signals, such as PD-1, LAG-3, CD160 and 2B4, and lose their functional effectiveness in a stepwise fashion.<sup>12,60</sup> In this study, we i.v. infected C57BL/6 mice with our OVA-expressing AdVova and phenotypically and functionally characterized OVA-specific CTLs. We observed mCTL expansion and mCTLs with defects in proliferation, IFN- $\gamma$  expression and cytotoxicity in the presence of AdVova-induced chronic infection, indicating that these OVA-specific mCTLs were functionally exhausted. These exhausted mCTLs upregulated their expression of inhibitory PD-1, PD-L1 and LAG-3, which is consistent with the CTL inflation and exhaustion observed in an LCMV clone 13-induced chronic infection model.<sup>12,60</sup> Therefore, our AdVova-infected mice may be utilized as a new chronic infection model to experimentally evaluate immunotherapeutics against chronic infection because of the commercial availability of the PE-H-2K<sup>b</sup>/OVA<sub>257-264</sub> tetramer, an immune reagent, allowing the detection of OVA-specific CTLs by flow cytometry.

A chronic infection with persisting pathogens can impair immune responses to unrelated infections and vaccines, and a dysfunctional immunity (a type of well-known bystander immunity in chronic infection) might be responsible for the increased susceptibility to various co-infections.<sup>49</sup> However, our current understanding of the bystander chronic infection is mainly based upon epidemiological evidence, with limited insight into the molecular mechanisms. DC defects in maturation, cytokine production and antigen presentation<sup>61-63</sup> and T-cell defects in proliferation<sup>64-66</sup> have been reported in animal models and humans with chronic infections. However, it is not clear whether the T-cell proliferation defect is intrinsic to T cells themselves or is derived from the functional deficiency of DCs. The upregulation of the inhibitory molecule PD-L1 was originally observed on splenocytes from chronically LCMV-infected mice, but the subset of immune cells expressing PD-L1 in splenocytes was not defined.<sup>36</sup> Later, reports confirmed that PD-L1 expression was high in the spleen tissues, especially on spleen CD11b<sup>+</sup>F4/80<sup>+</sup> macrophages and B220<sup>+</sup>CD19<sup>+</sup> B cells, but low in the bone marrow.<sup>67</sup> In our study, we demonstrate that naive CD8<sup>+</sup> T lymphocytes upregulate their expression of the inhibitory molecule PD-L1 and the immunoglobulin-like co-inhibitory receptor BTLA<sup>68</sup> and overexpress T-cell anergy-associated Grail and Itch molecules,<sup>69</sup> suggesting that these cells may become anergic in the presence of chronic infection. In addition, we show that during chronic infection, naive CD8<sup>+</sup> T cells also express cell surface CD40, which is absent on WT naive CD8<sup>+</sup> T cells. Naive CD8<sup>+</sup> T-cell anergy in our chronic infection model is further confirmed by showing that these naive CD8<sup>+</sup> T cells



have some degree of proliferation defect both in *in vitro* and *in vivo*. Therefore, our study is the first report demonstrating that naive CD8<sup>+</sup> T-cell anergy is responsible for a naive T-cell proliferation defect during chronic infection, thus revealing a new mechanism of CD8<sup>+</sup> T-cell anergy during the well-known bystander immunity in chronic infection. Nevertheless, the molecular mechanism for naive T-cell anergy in chronic infection needs to be further elucidated. Interestingly, our OVA-*Texo* vaccine, but not the DCova vaccine, is capable of counteracting naive T-cell anergy associated with chronic infection.

Co-stimulation with CD40L and inflammatory cytokines such as IL-2 and TNF- $\alpha$  has been reported to counteract T-cell anergy and tolerance.<sup>53</sup> To assess a potential molecular mechanism for the counteraction of T-cell anergy by OVA-*Texo*, we prepared a panel of OVA-*Texo* vaccines, OVA-*Texo*(IL-2<sup>-/-</sup>), OVA-*Texo*(TNF- $\alpha$ <sup>-/-</sup>) and OVA-*Texo*(CD40L<sup>-/-</sup>), which are deficient in IL-2, TNF- $\alpha$  or CD40L, respectively, and compared the OVA-specific CTL responses in AdV-infected B6 mice vaccinated with each of these preparations. We demonstrate here that the deficiency in CD40L alone, but not in other signaling components of the OVA-*Texo* vaccine, nearly completely abolishes its stimulatory effect on T-cell proliferation in our model of chronic infection, indicating that CD40L signaling has a central role in counteracting naive CD8<sup>+</sup> T-cell anergy. This was also supported by our experiments, showing that treatment with an antagonistic anti-CD40L antibody significantly reduced the stimulatory effect of OVA-*Texo* on T-cell proliferation. When considered together with our new finding that during chronic infection, naive CD8<sup>+</sup> T cells express cell surface CD40, these data allow us to speculate that CD40L has a central role in counteracting the anergy of naive CD40-expressing CD8<sup>+</sup> T cells via CD40/CD40L-initiated signaling.

CD40 signaling was originally found to activate and license DCs that then provide second signals to naive CD8<sup>+</sup> T cells upon antigen presentation.<sup>70-72</sup> We have previously demonstrated that CD40L signaling by our OVA-*Texo* vaccine did not enhance CTL priming, but promoted memory CTL development in WT B6 mice.<sup>39</sup> To assess a potential role of co-stimulatory CD40L-initiated signaling in the OVA-*Texo*-induced conversion of CTL exhaustion, we immunized AdVova-infected mice with OVA-*Texo*(CD40L<sup>-/-</sup>) cells lacking CD40L. We demonstrate that the absence of CD40L in the OVA-*Texo* vaccine strongly decreases its stimulating effect on CTL proliferation and its converting effect on CTL exhaustion in chronic infection, indicating that CD40L signaling has a crucial role in converting CD40-expressing CTL exhaustion in chronic infection. Therefore, we speculate that the OVA-*Texo*-induced conversion of CTL exhaustion occurs through breaking exhaustion via CD40L signaling, leading to an increased number of CTLs. Combined stimulation with exosomal OVA-specific peptide/MHC-I (pMHC-1), CD80 molecules, and cellular cytokines derived from OVA-*Texo* cells may contribute to the stimulation of CTLs independent of host DCs and CD4<sup>+</sup> T-cell help. Importantly, our data suggest that our Gag-specific

T-cell-based vaccine may also convert CTL exhaustion in HIV-1 patients with dysfunctional DCs and CD4<sup>±</sup> T-cell deficiency.<sup>7-10</sup>

The inhibitory PD-1 molecule is expressed on active T cells following TCR engagement and then declines. During chronic infection, PD-1 expression is sustained on CTLs due to persistent antigen stimulation, leading to CTL exhaustion. It has been demonstrated that PD-1 suppresses T-cell functions by antagonizing TCR signaling by recruiting phosphatases<sup>73,74</sup> and modulating the Ras and the PI3K/Akt/mTORC1 pathways regulating T-cell cycle, metabolism, proliferation and effector function,<sup>75,76</sup> leading to CTL exhaustion. It has also been shown that CD40L stimulates T-cell activation by inducing the recruitment of adaptor proteins, including the TNF receptor-associated factor, leading to the activation of the PI3K/Akt/mTORC1 pathway.<sup>56</sup> To assess whether the OVA-*Texo* vaccine activates the PI3K/Akt/mTORC1 pathway, we analyzed CTLs for the intracellular expression of molecules associated with this signaling cascade. Our experiments demonstrate that after immunization of chronically AdVova-infected mice with the OVA-*Texo* vaccine, the OVA-specific CTLs upregulate the expression or phosphorylation of pI3K, mTORC1-regulated pS6, pEIF4E and T-bet, which control T-cell activation, and increase the expression of a protein associated with cell cycle progression, Ki67. This strongly suggests that the conversion of CTL exhaustion by the OVA-*Texo* vaccine may occur via the activation of the PI3K/Akt/mTORC1 pathway. This is further supported by our data showing that the treatment of CTLs purified from chronically infected mice with an inhibitor of the mTORC1 pathway, rapamycin, significantly reduces their proliferation upon the OVA-*Texo* boost. Our data thus provide the first evidence that our novel T-cell-based vaccine is capable of converting CTL exhaustion in chronic infection, either mostly or at least in part via its CD40L-induced signaling through the mTORC1 pathway.

CD8<sup>+</sup> CTLs are important effector T cells capable of directly destroying HIV-1-infected cells, and they have a critical role in controlling HIV-1 proliferation and disease progression even in the absence of neutralizing antibodies.<sup>77,78</sup> Recently, efforts to purge latent reservoirs have focused on reactivating latent proviruses without inducing global T-cell activation.<sup>79</sup> Stimulation of HIV-1-specific CTLs has been reported to facilitate the elimination of latent viral reservoirs.<sup>80,81</sup> In this study, we demonstrated that HIV-1 Gag-specific, exosome-targeted, T-cell-based vaccine Gag-*Texo* is capable of inducing therapeutic immunity against Gag-expressing tumors during chronic infection, suggesting that our Gag-*Texo* vaccine may also induce the responses of CTLs that destroy HIV-1-infected cells. Humanized mouse models with HIV-1 infection, which mimic the immunopathology in HIV-1-infected human patients, have become useful for studying the mechanisms of HIV-1 immunopathogenesis and for developing novel immune-based therapies.<sup>82,83</sup> We are also planning to develop an HIV-1-infected humanized mouse model to further assess the potential therapeutic efficacy of our Gag-*Texo* vaccine.

In summary, our data demonstrate that our novel antigen-specific, exosome-targeted, T-cell-based vaccine is capable of counteracting the anergy of naive CD40-expressing CD8<sup>+</sup> T cells and converts the exhaustion of CD40-expressing CTLs independent of DCs and CD4<sup>+</sup> T cells. It achieves these effects by acting through CD40L-triggered signaling, inducing the activation of the mTORC1 pathway and thus efficiently stimulating Gag-specific therapeutic immunity in the presence of chronic infection. Therefore, this study is likely to produce a strong impact on the development of new therapeutic vaccines against HIV-1 and other chronic infectious diseases.

## CONFLICT OF INTEREST

The authors declare no conflict of interest.

## ACKNOWLEDGEMENTS

We thank Mark Boyd for help in flow cytometric analyses. This work was supported by a Canadian Institute of Health Research (CIHR) grant (OCH 126276).

- Sallusto F, Lanzavecchia A, Araki K, Ahmed R. From vaccines to memory and back. *Immunity* 2010; **33**: 451–463.
- Murali-Krishna K, Altman JD, Suresh M, Sourdive DJ, Zajac AJ, Miller JD *et al*. Counting antigen-specific CD8 T cells: a reevaluation of bystander activation during viral infection. *Immunity* 1998; **8**: 177–187.
- Butz EA, Bevan MJ. Massive expansion of antigen-specific CD8<sup>+</sup> T cells during an acute virus infection. *Immunity* 1998; **8**: 167–175.
- Krammer PH, Arnold R, Lavrik IN. Life and death in peripheral T cells. *Nat Rev Immunol* 2007; **7**: 532–542.
- Harty JT, Badovinac VP. Shaping and reshaping CD8<sup>+</sup> T-cell memory. *Nat Rev Immunol* 2008; **8**: 107–119.
- Kaech SM, Wherry EJ, Ahmed R. Effector and memory T-cell differentiation: implications for vaccine development. *Nat Rev Immunol* 2002; **2**: 251–262.
- Harari A, Petitpierre S, Vallelian F, Pantaleo G. Skewed representation of functionally distinct populations of virus-specific CD4 T cells in HIV-1-infected subjects with progressive disease: changes after anti-retroviral therapy. *Blood* 2004; **103**: 966–972.
- Pantaleo G, Koup RA. Correlates of immune protection in HIV-1 infection: what we know, what we don't know, what we should know. *Nat Med* 2004; **10**: 806–810.
- Donaghy H, Pozniak A, Gazzard B, Qazi N, Gilmour J, Gotch F *et al*. Loss of blood CD11c(+) myeloid and CD11c(-) plasmacytoid dendritic cells in patients with HIV-1 infection correlates with HIV-1 RNA virus load. *Blood* 2001; **98**: 2574–2576.
- Pacanowski J, Kahi S, Baillet M, Lebon P, Deveau C, Goujard C *et al*. Reduced blood CD123+ (lymphoid) and CD11c+ (myeloid) dendritic cell numbers in primary HIV-1 infection. *Blood* 2001; **98**: 3016–3021.
- Zajac AJ, Blattman JN, Murali-Krishna K, Sourdive DJ, Suresh M, Altman JD *et al*. Viral immune evasion due to persistence of activated T cells without effector function. *J Exp Med* 1998; **188**: 2205–2213.
- Blackburn SD, Shin H, Haining WN, Zou T, Workman CJ, Polley A *et al*. Coregulation of CD8<sup>+</sup> T cell exhaustion by multiple inhibitory receptors during chronic viral infection. *Nat Immunol* 2009; **10**: 29–37.
- Fischbach MA, Bluestone JA, Lim WA. Cell-based therapeutics: the next pillar of medicine. *Sci Transl Med* 2013; **5**: 179.
- Lapenta C, Santini SM, Logozzi M, Spada M, Andreotti M, Di Pucchio T *et al*. Potent immune response against HIV-1 and protection from virus challenge in hu-PBL-SCID mice immunized with inactivated virus-pulsed dendritic cells generated in the presence of IFN- $\alpha$ . *J Exp Med* 2003; **198**: 361–367.
- Carbonneil C, Aouba A, Burgard M, Cardinaud S, Rouzioux C, Langlade-Demoyen P *et al*. Dendritic cells generated in the presence of granulocyte-macrophage colony-stimulating factor and IFN- $\alpha$  are potent inducers of HIV-specific CD8 T cells. *AIDS* 2003; **17**: 1731–1740.
- Villamide-Herrera L, Ignatius R, Eller MA, Wilkinson K, Griffin C, Mehlhop E *et al*. Macaque dendritic cells infected with SIV-recombinant canarypox *ex vivo* induce SIV-specific immune responses in vivo. *AIDS Res Hum Retroviruses* 2004; **20**: 871–884.
- Lu W, Arraes LC, Ferreira WT, Andrieu JM. Therapeutic dendritic-cell vaccine for chronic HIV-1 infection. *Nat Med* 2004; **10**: 1359–1365.
- Garcia F, Lejeune M, Climent N, Gil C, Alcamí J, Morente V *et al*. Therapeutic immunization with dendritic cells loaded with heat-inactivated autologous HIV-1 in patients with chronic HIV-1 infection. *J Infect Dis* 2005; **191**: 1680–1685.
- Garcia F, Routy JP. Challenges in dendritic cells-based therapeutic vaccination in HIV-1 infection Workshop in dendritic cell-based vaccine clinical trials in HIV-1. *Vaccine* 2011; **29**: 6454–6463.
- Garcia F, Climent N, Assoumou L, Gil C, González N, Alcamí J *et al*. A therapeutic dendritic cell-based vaccine for HIV-1 infection. *J Infect Dis* 2011; **203**: 473–478.
- Garcia F, Plana M, Climent N, Leon A, Gatell JM, Gallart T. Dendritic cell based vaccines for HIV infection: the way ahead. *Hum Vaccin Immunother* 2013; **9**: 2445–2452.
- Xiang J, Huang H, Liu Y. A new dynamic model of CD8<sup>+</sup> T effector cell responses via CD4<sup>+</sup> T helper-antigen-presenting cells. *J Immunol* 2005; **174**: 7497–7505.
- Hao S, Liu Y, Yuan J, Zhang X, He T, Wu X *et al*. Novel exosome-targeted CD4<sup>+</sup> T cell vaccine counteracting CD4<sup>+</sup>25<sup>+</sup> regulatory T cell-mediated immune suppression and stimulating efficient central memory CD8<sup>+</sup> CTL responses. *J Immunol* 2007; **179**: 2731–2740.
- Hao S, Yuan J, Xiang J. Nonspecific CD4(+) T cells with uptake of antigen-specific dendritic cell-released exosomes stimulate antigen-specific CD8(+) CTL responses and long-term T cell memory. *J Leukoc Biol* 2007; **82**: 829–838.
- Nanjundappa RH, Wang R, Xie Y, Umeshappa CS, Chibbar R, Wei Y *et al*. GP120-specific exosome-targeted T cell-based vaccine capable of stimulating DC- and CD4(+) T-independent CTL responses. *Vaccine* 2011; **29**: 3538–3547.
- Nanjundappa RH, Wang R, Xie Y, Umeshappa CS, Xiang J. Novel CD8<sup>+</sup> T cell-based vaccine stimulates Gp120-specific CTL responses leading to therapeutic and long-term immunity in transgenic HLA-A2 mice. *Vaccine* 2012; **30**: 3519–3525.
- Liu Y, Li F, Liu Y, Hong K, Meng X, Chen J *et al*. HIV fragment gag vaccine induces broader T cell response in mice. *Vaccine* 2011; **29**: 2582–2589.
- Wang R, Xie Y, Zhao T, Tan X, Xu J, Xiang J. HIV-1 Gag-specific exosome-targeted T cell-based vaccine stimulates effector CTL responses leading to therapeutic and long-term immunity against Gag/HLA-A2-expressing B16 melanoma in transgenic HLA-A2 mice. *Trials Vaccinol* 2014; **3**: 19–25.
- Wang R, Freywald A, Chen Y, Xu J, Tan X, Xiang J. Transgenic 4-1BBL-engineered vaccine stimulates potent Gag-specific therapeutic and long-term immunity via increased priming of CD44CD62L IL-7R CTLs with up- and downregulation of anti- and pro-apoptosis genes. *Cell Mol Immunol* 2015; **12**: 456–465.
- Chen L, Flies DB. Molecular mechanisms of T cell co-stimulation and co-inhibition. *Nat Rev Immunol* 2013; **13**: 227–242.
- Krebs P, Scandella E, Odermatt B, Ludewig B. Rapid functional exhaustion and deletion of CTL following immunization with recombinant adenovirus. *J Immunol* 2005; **174**: 4559–4566.
- Rodig N, Ryan T, Allen JA, Pang H, Grabie N, Chernova T *et al*. Endothelial expression of PD-L1 and PD-L2 down-regulates CD8<sup>+</sup> T cell activation and cytotoxicity. *Eur J Immunol* 2003; **33**: 3117–3126.
- Chen Y, Xie Y, Chan T, Sami A, Ahmed S, Liu Q *et al*. Adjuvant effect of HER-2/neu-specific adenoviral vector stimulating CD8(+) T and natural killer cell responses on anti-HER-2/neu antibody therapy for well-established breast tumors in HER-2/neu transgenic mice. *Cancer Gene Ther* 2011; **18**: 489–499.
- Yajima T, Nishimura H, Sad S, Shen H, Kuwano H, Yoshikai Y. A novel role of IL-15 in early activation of memory CD8<sup>+</sup> CTL after reinfection. *J Immunol* 2005; **174**: 3590–3597.

- 35 Shi M, Hao S, Chan T, Xiang J. CD4(+) T cells stimulate memory CD8(+) T cell expansion via acquired pMHC I complexes and costimulatory molecules, and IL-2 secretion. *J Leukoc Biol* 2006; **80**: 1354–1363.
- 36 Barber DL, Wherry EJ, Masopust D, Zhu B, Allison JP, Sharpe AH et al. Restoring function in exhausted CD8 T cells during chronic viral infection. *Nature* 2006; **439**: 682–687.
- 37 Abe BT, Shin DS, Mocholi E, Macian F. NFAT1 supports tumor-induced anergy of CD4(+) T cells. *Cancer Res* 2012; **72**: 4642–4651.
- 38 Umeshappa CS, Xie Y, Xu S, Nanjundappa RH, Freywald A, Deng Y et al. Th cells promote CTL survival and memory via acquired pMHC-I and endogenous IL-2 and CD40L signaling and by modulating apoptosis-controlling pathways. *PLoS One* 2013; **8**: e64787.
- 39 Xie Y, Wang L, Freywald A, Qureshi M, Chen Y, Xiang J. A novel T cell-based vaccine capable of stimulating long-term functional CTL memory against B16 melanoma via CD40L signaling. *Cell Mol Immunol* 2013; **10**: 72–77.
- 40 He S, Kato K, Jiang J, Wahl DR, Mineishi S, Fisher EM et al. Characterization of the metabolic phenotype of rapamycin-treated CD8 + T cells with augmented ability to generate long-lasting memory cells. *PLoS One* 2011; **6**: e20107.
- 41 Ahmed KA, Wang L, Munegowda MA, Mulligan SJ, Gordon JR, Griebel P et al. Direct in vivo evidence of CD4+ T cell requirement for CTL response and memory via pMHC-I targeting and CD40L signaling. *J Leukoc Biol* 2012; **92**: 289–300.
- 42 Ankathatti Munegowda M, Deng Y, Mulligan SJ, Xiang J. Th17 and Th17-stimulated CD8(+) T cells play a distinct role in Th17-induced preventive and therapeutic antitumor immunity. *Cancer Immunol Immunother* 2011; **60**: 1473–1484.
- 43 Tatsis N, Fitzgerald JC, Reyes-Sandoval A, Harris-McCoy KC, Hensley SE, Zhou D et al. Adenoviral vectors persist in vivo and maintain activated CD8+ T cells: implications for their use as vaccines. *Blood* 2007; **110**: 1916–1923.
- 44 Yang TC, Millar J, Groves T, Grinshtein N, Parsons R, Takenaka S et al. The CD8+ T cell population elicited by recombinant adenovirus displays a novel partially exhausted phenotype associated with prolonged antigen presentation that nonetheless provides long-term immunity. *J Immunol* 2006; **176**: 200–210.
- 45 Yang ZR, Wang HF, Zhao J, Peng YY, Wang J, Guinn BA et al. Recent developments in the use of adenoviruses and immunotoxins in cancer gene therapy. *Cancer Gene Ther* 2007; **14**: 599–615.
- 46 Finn JD, Bassett J, Millar JB, Grinshtein N, Yang TC, Parsons R et al. Persistence of transgene expression influences CD8+ T-cell expansion and maintenance following immunization with recombinant adenovirus. *J Virol* 2009; **83**: 12027–12036.
- 47 Holst PJ, Orskov C, Thomsen AR, Christensen JP. Quality of the transgene-specific CD8+ T cell response induced by adenoviral vector immunization is critically influenced by virus dose and route of vaccination. *J Immunol* 2010; **184**: 4431–4439.
- 48 Kaufman DR, Bivas-Benita M, Simmons NL, Miller D, Barouch DH. Route of adenovirus-based HIV-1 vaccine delivery impacts the phenotype and trafficking of vaccine-elicited CD8+ T lymphocytes. *J Virol* 2010; **84**: 5986–5996.
- 49 Stelekati E, Wherry EJ. Chronic bystander infections and immunity to unrelated antigens. *Cell Host Microbe* 2012; **12**: 458–469.
- 50 Deng A, Chen S, Li Q, Lyu SC, Clayberger C, Krensky AM. Granulysin, a cytolytic molecule, is also a chemoattractant and proinflammatory activator. *J Immunol* 2005; **174**: 5243–5248.
- 51 Brossart P, Zobywalski A, Grunebach F, Behnke L, Stuhler G, Reichardt VL et al. Tumor necrosis factor alpha and CD40 ligand antagonize the inhibitory effects of interleukin 10 on T-cell stimulatory capacity of dendritic cells. *Cancer Res* 2000; **60**: 4485–4492.
- 52 Pasare C, Medzhitov R. Toll pathway-dependent blockade of CD4 +CD25+ T cell-mediated suppression by dendritic cells. *Science* 2003; **299**: 1033–1036.
- 53 Valencia X, Stephens G, Goldbach-Mansky R, Wilson M, Shevach EM, Lipsky PE. TNF downmodulates the function of human CD4+CD25hi T-regulatory cells. *Blood* 2006; **108**: 253–261.
- 54 Bevan MJ. Helping the CD8(+) T-cell response. *Nat Rev Immunol* 2004; **4**: 595–602.
- 55 Dispirito JR, Shen H. Histone acetylation at the single-cell level: a marker of memory CD8+ T cell differentiation and functionality. *J Immunol* 2010; **184**: 4631–4636.
- 56 Elgueta R, Benson MJ, de Vries VC, Wasiuk A, Guo Y, Noelle RJ. Molecular mechanism and function of CD40/CD40L engagement in the immune system. *Immunol Rev* 2009; **229**: 152–172.
- 57 Yang TC, Millar JB, Grinshtein N, Bassett J, Finn J, Bramson JL. T-cell immunity generated by recombinant adenovirus vaccines. *Expert Rev Vaccines* 2007; **6**: 347–356.
- 58 Bassett JD, Swift SL, Bramson JL. Optimizing vaccine-induced CD8(+) T-cell immunity: focus on recombinant adenovirus vectors. *Expert Rev Vaccines* 2011; **10**: 1307–1319.
- 59 Wherry EJ. T cell exhaustion. *Nat Immunol* 2011; **12**: 492–499.
- 60 Yi JS, Cox MA, Zajac AJ. T-cell exhaustion: characteristics, causes and conversion. *Immunology* 2010; **129**: 474–481.
- 61 van Riet E, Hartgers FC, Yazdanbakhsh M. Chronic helminth infections induce immunomodulation: consequences and mechanisms. *Immunobiology* 2007; **212**: 475–490.
- 62 Su Z, Segura M, Morgan K, Loredó-Osti JC, Stevenson MM. Impairment of protective immunity to blood-stage malaria by concurrent nematode infection. *Infect Immun* 2005; **73**: 3531–3539.
- 63 Metenou S, Kovacs M, Dembele B, Coulibaly YI, Klion AD, Nutman TB. Interferon regulatory factor modulation underlies the bystander suppression of malaria antigen-driven IL-12 and IFN-gamma in filaria-malaria co-infection. *Eur J Immunol* 2012; **42**: 641–650.
- 64 Yin J, Vahey MT, Dai A, Lewis MG, Arango T, Yalley-Ogunro J et al. Plasmodium inui infection reduces the efficacy of a simian immunodeficiency virus DNA vaccine in a rhesus macaque model through alteration of the vaccine-induced immune response. *J Infect Dis* 2012; **206**: 523–533.
- 65 Elias D, Wolday D, Akuffo H, Petros B, Bronner U, Britton S. Effect of deworming on human T cell responses to mycobacterial antigens in helminth-exposed individuals before and after bacille Calmette-Guerin (BCG) vaccination. *Clin Exp Immunol* 2001; **123**: 219–225.
- 66 Moorman JP, Zhang CL, Ni L, Ma CJ, Zhang Y, Wu XY et al. Impaired hepatitis B vaccine responses during chronic hepatitis C infection: involvement of the PD-1 pathway in regulating CD4(+) T cell responses. *Vaccine* 2011; **29**: 3169–3176.
- 67 Blackburn SD, Crawford A, Shin H, Polley A, Freeman GJ, Wherry EJ. Tissue-specific differences in PD-1 and PD-L1 expression during chronic viral infection: implications for CD8 T-cell exhaustion. *J Virol* 2010; **84**: 2078–2089.
- 68 Derre L, Rivals JP, Jandus C, Pastor S, Rimoldi D, Romero P et al. BTLA mediates inhibition of human tumor-specific CD8+ T cells that can be partially reversed by vaccination. *J Clin Invest* 2010; **120**: 157–167.
- 69 Wells AD. New insights into the molecular basis of T cell anergy: anergy factors, avoidance sensors, and epigenetic imprinting. *J Immunol* 2009; **182**: 7331–7341.
- 70 Ridge JP, Di Rosa F, Matzinger P. A conditioned dendritic cell can be a temporal bridge between a CD4+ T-helper and a T-killer cell. *Nature* 1998; **393**: 474–478.
- 71 Bennett SR, Carbone FR, Karamalis F, Flavell RA, Miller JF, Heath WR. Help for cytotoxic-T-cell responses is mediated by CD40 signalling. *Nature* 1998; **393**: 478–480.
- 72 Schoenberger SP, Toes RE, van der Voort EI, Offringa R, Melief CJ. T-cell help for cytotoxic T lymphocytes is mediated by CD40-CD40L interactions. *Nature* 1998; **393**: 480–483.
- 73 Sheppard KA, Fitz LJ, Lee JM, Benander C, George JA, Wooters J et al. PD-1 inhibits T-cell receptor induced phosphorylation of the ZAP70/CD3zeta signalosome and downstream signaling to PKCtheta. *FEBS Lett* 2004; **574**: 37–41.
- 74 Yokosuka T, Takamatsu M, Kobayashi-Imanishi W, Hashimoto-Tane A, Azuma M, Saito T. Programmed cell death 1 forms negative costimulatory microclusters that directly inhibit T cell receptor signaling by recruiting phosphatase SHP2. *J Exp Med* 2012; **209**: 1201–1217.
- 75 Parry RV, Chemnitz JM, Frauwirth KA, Lanfranco AR, Braunstein I, Kobayashi SV et al. CTLA-4 and PD-1 receptors inhibit T-cell activation by distinct mechanisms. *Mol Cell Biol* 2005; **25**: 9543–9553.
- 76 Patsoukis N, Brown J, Petkova V, Liu F, Li L, Boussiotis VA. Selective effects of PD-1 on Akt and Ras pathways regulate molecular components of the cell cycle and inhibit T cell proliferation. *Sci Signal* 2012; **5**: ra46.
- 77 Kawada M, Tsukamoto T, Yamamoto H, Takeda A, Igarashi H, Watkins DI et al. Long-term control of simian immunodeficiency virus replication with central memory CD4+ T-cell preservation after



- nonsterile protection by a cytotoxic T-lymphocyte-based vaccine. *J Virol* 2007; **81**: 5202–5211.
- 78 McKinnon LR, Kaul R, Kimani J, Nagelkerke NJ, Wachhi C, Fowke KR *et al*. HIV-specific CD8+ T-cell proliferation is prospectively associated with delayed disease progression. *Immunol Cell Biol* 2012; **90**: 346–351.
- 79 Xing S, Bullen CK, Shroff NS, Shan L, Yang HC, Manucci JL *et al*. Disulfiram reactivates latent HIV-1 in a Bcl-2-transduced primary CD4+ T cell model without inducing global T cell activation. *J Virol* 2011; **85**: 6060–6064.
- 80 Redel L, Le Douce V, Cherrier T, Marban C, Janossy A, Aunis D *et al*. HIV-1 regulation of latency in the monocyte-macrophage lineage and in CD4+ T lymphocytes. *J Leukoc Biol* 2010; **87**: 575–588.
- 81 Shan L, Deng K, Shroff NS, Durand CM, Rabi SA, Yang HC *et al*. Stimulation of HIV-1-specific cytolytic T lymphocytes facilitates elimination of latent viral reservoir after virus reactivation. *Immunity* 2012; **36**: 491–501.
- 82 Ito R, Takahashi T, Katano I, Ito M. Current advances in humanized mouse models. *Cell Mol Immunol* 2012; **9**: 208–214.
- 83 Zhang L, Su L. HIV-1 immunopathogenesis in humanized mouse models. *Cell Mol Immunol* 2012; **9**: 237–244.

Supplementary Information for this article can be found on the *Cellular & Molecular Immunology* website (<http://www.nature.com/cmi>)